sustainability

MDPI

Article

Assessing the Applicability of Biodegradable Film Mulching in Northwest China Based on Comprehensive Benefits Study

Liyuan Bo [1,2], Xiaomin Mao [1,2,*] and Yali Wang [1,2]

1 Center for Agricultural Water Research in China, China Agricultural University, Beijing 100083, China
2 National Field Scientific Observation and Research Station on Efficient Water Use of Oasis Agriculture in Wuwei of Gansu Province, Wuwei 733000, China
* Correspondence: maoxiaomin@cau.edu.cn; Tel./Fax: +86-10-62738498

Abstract: Biodegradable film is a promising alternative to polyethylene film in arid regions, but its use is usually inhibited by its high cost and elusive effects on soil and crop yield. A two-year field experiment was carried out to explore the impact of biodegradable film on soil hydrothermal dynamics, yield, water productivity and economic benefits under three irrigation strategies (full, medium and low irrigation amount) compared with non-mulching and polyethylene film. The comprehensive benefits (economic, technical and ecological) of different film mulching patterns were evaluated using analytic hierarchy process and gray relational analysis methods. The results indicated that increasing irrigation amount could accelerate the degradation of the biodegradable film, with the highest film weight loss rate of 38.8% obtained under full irrigation. Film mulching could mitigate the negative impact of water deficit on crop yield, with the yield of biodegradable film and polyethylene film enhanced by 11.6% and 18.6% compared with non-mulching under low irrigation. Although polyethylene film showed the highest economic benefits, non-mulching showed the highest comprehensive benefits. Only when the price of biodegradable film material dropped to less than 1.37 times that of polyethylene film did the economic benefit of biodegradable film outcompete non-mulching and become a more acceptable and promising farming solution to boosting environmental sustainability.

Keywords: biodegradable film; deficit irrigation; yield; economic benefits; sustainable agriculture; AHP-GRA

Citation: Bo, L.; Mao, X.; Wang, Y. Assessing the Applicability of Biodegradable Film Mulching in Northwest China Based on Comprehensive Benefits Study. *Sustainability* **2022**, *14*, 10584. https://doi.org/10.3390/su141710584

Academic Editor: Jan Hopmans

Received: 15 July 2022
Accepted: 20 August 2022
Published: 25 August 2022

1. Introduction

Plastic film mulching (PM) can significantly improve crop yield, water productivity and profitability [1] due to its impact on soil temperature enhancement [2], soil evaporation and weeds suppression [3,4]. A commonly used plastic film for mulching is polyethylene (PE), which is low in cost and convenient for machine paving [5,6]. China consumes about 2.45 million tons of PE [7], while Western Europe consumes about 0.57 million tons annually [8]. Currently, PE is ranked as the fourth most necessary agricultural material in China, behind chemical fertilizer, seed and pesticide [9].

Completely recycling residual PE film, in spite of the advantages, is challenging because of the difficulty of mechanical recycling and the lack of a related compulsory policy [10], while persistent PE residue in the soil could cause an irreversible and negative impact on the field ecosystem [11]. For example, PE residue may negatively affect water and nutrition absorption in the root system, seed emergence and crop yield [12], whereas burning PE residue produces persistent organic pollutants known as furans and dioxins [13]. Therefore, PE mulch use in agriculture is facing increasing environmental and social pressures. Overcoming the negative effects of film mulching is essential for building a sustainable and environmentally friendly agroecosystem.

In recent years, non-polluting and environmentally friendly degradable agricultural films have been developed as a promising alternative to PE film [14]. Degradable agricultural films are generally classified into two types, photodegradable films and biodegradable films [8]. Previous studies showed that photodegradation would stop degradation if it was covered by the soil or crop canopy; thus, the degradation rate was difficult to control [15], which restricted its extensive application. Biodegradable films are produced from a biodegradable PE starch plastic substance that can be degraded by natural microorganisms such as bacteria, fungi and algae [16]. Their final metabolites are CO_2 and H_2O, without any pollution to the ecological environment [17,18]. Previous studies show that biodegradable films could increase soil temperature, maintain soil moisture and restrain evaporation [19], achieving higher crop yields and water productivity compared to bare soil [19,20].

Yet, biodegradable films may face uncertainty in the emergence of film cracks under complex environmental conditions, which may bring negative impacts on crop growth. Previous research indicated that crop yields under biodegradable film mulching (BM) were generally lower than under PE film mulching because the former was less effective at conserving soil water and heat [21,22]. Thus, BM's effect on hydrothermal soil conditions, especially after degradation, needs to be investigated. In arid and semi-arid areas, mulching and deficit irrigation are widely used to alleviate the contradiction between the water scarcity and yield improvement [2]. Deficit irrigation could promote plant growth and development, stimulate root activity, maintain or increase plant yield, influence product quality, improve nutrient use efficiency and enhance plant acclimatization [23–25]. Therefore, it is necessary to elucidate the coupling effects of biodegradable film and different irrigation strategies on the soil′s hydrothermal and degradation characteristics and their effects on crop yield and economic efficiency.

Additionally, the high price of biodegradable film is one of the factors limiting its large-scale promotion in China. Thus, the economic benefits of crops mulched by biodegradable film have been questioned. Some studies have examined the economic profit of biodegradable film mulching and PE film mulching based on material cost and crop yield [26–28]. However, among biodegradable film's key characteristics is its advantage in reducing environmental pollution. It is necessary, then, to evaluate the comprehensive benefits of biodegradable film in terms of economic [28,29], technological and ecological benefits when attempting to improve understanding about building sustainable and environmentally friendly agroecosystem.

Evaluation methods such as analytic hierarchy process (AHP), gray relational analysis (GRA), fuzzy comprehensive evaluation (FCE), synthetical scored method and statistical assessment are widely used to identify weights for system comprehensive evaluation indicators [30–32]. The AHP method was proposed by Saaty [33] and is widely used in analysis, management and evaluation; it is a decision-making method that combines qualitative and quantitative analysis and is used to calculate the weight of evaluation index system [34,35]. GRA is a method in grey system theory, a quantitative approach describing the degree of correlation between objects and factors [36,37]. The AHP-GRE comprehensive evaluation method is scientific and comprehensive in calculating the weights of agroecosystem evaluation indicators [38,39].

The objectives of this paper were to (i) explore the coupling effects of different film mulching patterns and irrigation strategies on the degradation characteristics, hydrothermal soil characteristics, maize yield, water productivity and economic benefits and (ii) construct a comprehensive benefits evaluation system for different mulching patterns and conduct an evaluation of their performance using the AHP-GRE method.

2. Materials and Methods

2.1. Experimental Site Description

The field experiment was established from May to September in 2020 and 2021 at the National Field Scientific Observation and Research Station on Efficient Water Use of Oasis Agriculture in Wuwei of Gansu Province of China (37°52′ N, 102°52′ E, altitude: 1581 m). The region is characterized by a typical continental temperate climate with the mean annual precipitation of 164 mm, average annual temperature of 8 °C and annual frost-free period of

150 d. Moreover, the sunshine duration is more than 3000 h, the mean annual pan evaporation is 2000 mm and the mean annual air cumulative temperature (>0 °C) is 3550 °C [4,40,41]. The groundwater table is 40~50 m below the ground surface. The soil is classified as a silty loam, with volumetric field capacity, permanent wilting point and dry bulk density of 0.32 m^3 m^{-3}, 0.10 m^3 m^{-3} and 1.53 ± 0.05 g cm^{-3}, respectively [42].

2.2. Experiment Design

In this experiment, Xianyu 335 (Gansu Dunhuang Seed Group Co., Ltd., Jiuquan, China), a major spring maize cultivar in the region, was planted on the farmland. This field experiment consists of three film mulching patterns (non-mulching (NM), transparent PE PM (Shuangxing Plastic Products Factory, Jining, China) and BM (Jin Hui Zhao Long High Technology Co., Ltd., Lvliang, China)) and three irrigation strategies (full irrigation amounts (FI), medium irrigation amounts (70% FI, MI) and low irrigation amounts (40% FI, LI), as listed in Table 1). The biodegradable film was made from polybutylene co-adipate co-terephthalate (PBAT) and polycaprolactone blended with starch. The FI was obtained by subtracting effective rainfall from crop water requirement (ET), which was calculated as the product of reference crop evapotranspiration and crop coefficient. The daily crop evapotranspiration was calculated with the Penman–Monteith equation [43], and the crop coefficient was obtained from a previous study from the same test area [4]. As listed in Table 1, irrigation intervals were about 10 days; hence, in the calculation of the full irrigation amount per irrigation, the total ET was the sum of ET in the previous 10 days. Each of the nine treatments had three replicates, and the 27 plots (each 8 m in length and 5.6 m in width) were arranged in a randomized block design (Figure 1).

Table 1. Irrigation amounts (mm) under different treatments during 2020 and 2021.

Years	Treatments	Irrigation Date (Month/Day) and Irrigation Amounts (mm)									Total Irrigation Amounts
2020		6/13	6/24	7/4	7/14	7/24	8/3	8/13	8/24	9/3	
	NM/PM/BM-FI	21.6	27	39.3	40.3	40.7	55.1	51.2	46.8	22.9	344.9
	NM/PM/BM-MI	15.1	18.9	27.5	28.2	28.5	38.6	35.9	32.7	16.1	241.5
	NM/PM/BM-LI	8.7	10.8	15.7	16.1	16.3	22.0	20.5	18.7	9.2	138.0
2021		6/11	6/21	7/1	7/10	7/20	7/29	8/8	8/17	8/29	
	NM/PM/BM-FI	16.0	21.3	35.8	47.5	49.1	56.5	52.6	44.0	36.4	359.2
	NM/PM/BM-MI	11.2	14.9	25.1	33.2	34.4	39.5	36.8	30.8	25.5	251.4
	NM/PM/BM-LI	6.4	8.5	14.3	19.0	19.7	22.6	21.1	17.6	14.5	143.7

The maize row and plant spacings were 40 cm and 25 cm, respectively. The drip line was placed between two rows of spring maize with a spacing of 80 cm. Drippers were located every 30 cm along the drip line, and the discharge rate was 2.5 L h^{-1}. All seeds were sown on 4 May 2020 and 30 April 2021, and maize was harvested on 16 September 2020 (NM treatment), 27 September 2020 (PM and BM treatments), 17 September 2021 (NM treatment) and 27 September 2021 (PM and BM treatments), respectively. During the experimental period, irrigation was conducted about every 10 days from 13 June 2020 (11 June 2021) to 3 September 2020 (27 August 2021). All plots received a basal dose of fertilizer before planting (375 kg·ha^{-1} $(NH_4)_2HPO_4$) and received the same amount of fertilizer at the jointing stage (525 kg·ha^{-1} CH_4N_2O) [44–47]. The corresponding treatment and field management of each plot were unchanged during the two experimental years.

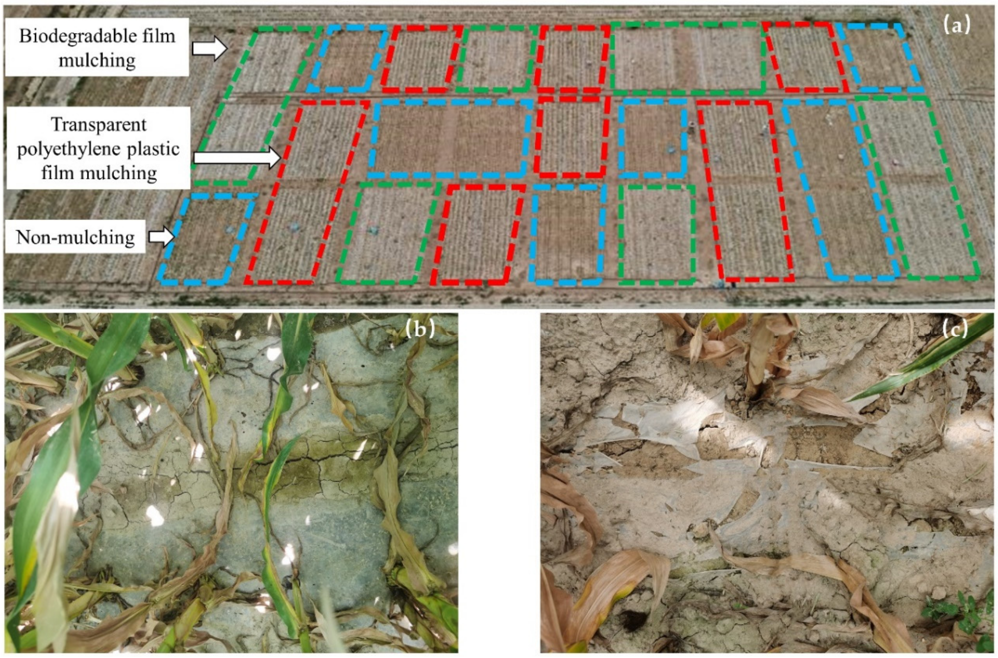

Figure 1. Overview of the experimental area and design: (**a**) a panoramic view of experimental area; (**b**) BM after harvest of maize; (**c**) PM after harvest of maize.

2.3. Sampling and Calculations

2.3.1. Biodegradability

Film degradation in the field was observed and recorded every 15 days after sowing (DAS) using a qualitative scale [48]. The film degradation process could be divided into five stages [49,50]. Stage I indicated that the film had begun to crack after the induction period; Stage II indicated that 25% of the film appeared to show tiny cracks; Stage III indicated that the cracks in the film were 2~2.5 cm wide, and the number of cracks increased; Stage IV indicated that the film was broken into little fragments, with no large pieces of film, and the cracks were uniform and reticular at this stage; Stage V indicated that almost no residual film piece existed on the soil surface and the film was degraded into fragments smaller than 4 × 4 cm^2.

After harvest, three sampling quadrats (0.6 m wide, 0.6 m long) were randomly selected in each plot, and the residual films on the soil surface were collected. All of the residual films were taken back to the laboratory and washed thoroughly in an ultrasonic cleaner (30 min). After air drying to a stable weight, the loss rate (Q_L, %) was calculated as:

$$Q_L = \frac{Q_0 - Q_1}{Q_0} \times 100\% \quad (1)$$

where Q_1 is the weight of the residual biodegradable film after harvest (g), and Q_0 is the weight of the biodegradable film before the experiment (g).

2.3.2. Soil Water Storage and Soil Temperature

A TRIME tube was placed in the middle of every plot. The soil profile was divided into five sampling intervals (including 0~20, 20~40, 40~60, 60~80 and 80~100 cm) for soil water content measurement using Time-Domain-Reflectometry (TRIME-PICO/PICO-BT, Imko GmbH, Ettlingen, Germany) every 3~7 d. It was calibrated with volumetric soil water content that was obtained based on mass soil water content from the oven drying method and the measured soil bulk density. The soil water storage of 1 m soil depth (*SWS*, mm) was calculated as follows:

$$SWS = \sum_{i=1}^{5} SWC_i \times H \quad (2)$$

where *SWC* is the volumetric soil water content (cm^3 cm^{-3}), i is soil layer number and H refers to the thickness of the soil layer (mm).

A set of temperature sensors connected with soil temperature recorders (HZ-TJ1, both sensors and recorders came from the Hezhong Bopu Technology Development Co., Ltd., Beijing, China) was placed in the middle of every treatment plot at soil depths of 5, 10 and 20 cm and monitored every 30 min. The mean daily soil temperature (T_s) was calculated based on the data series sampled each day. The measurement spot of T_s remains unchanged in two maize-growing seasons.

2.3.3. Growth Stages

The crop growing period can be divided into four distinct growth stages (i.e., initial (from planting date to approximately 10% ground cover), development (from 10% ground cover to effective full cover), mid-season (from effective full cover to the start of maturity) and late season (from the start of maturity to harvest or full senescence)) [43]. The date on which 70% of the plants in each plot showed the main characteristics of a particular growth stage was used to demarcate their entry into that growth stage.

2.3.4. Grain Yield and Water Productivity

At maturity, the 10 consecutive maize ears were hand-harvested from the center of each plot to measure the maize grain yield, which was expressed at a water content of 13% [26,51].

The water productivity (*WP*, kg m^{-3}) was calculated as [52]:

$$WP = 10 \times \frac{Y}{ET} \tag{3}$$

where Y is the grain yield of maize (kg ha^{-1}) and ET is the total evapotranspiration over the growing season in each year (mm, i.e., 10 m^3 ha^{-1}). ET can be calculated using the soil water balance equation as:

$$ET = P + I + SWS\_s - SWS\_h - R - D + W \tag{4}$$

where P is rainfall (mm), I is the amount of irrigation (mm) and SWS_s and SWS_h are soil water storage in the root zone (here 0~100 cm soil depth) at sowing and harvest, respectively. R is surface runoff (mm), D is the deep percolation (mm) and W is the upward soil water flux to the root zone (mm). This experimental site is flat with no large precipitation during maize growing seasons, and the groundwater table depth is over 40~50 m. Therefore, R, D and W were negligible. Equation (4) is simplified as follows:

$$ET = P + I + SWS\_s - SWS\_h \tag{5}$$

2.3.5. Profitability Analysis

In this study, an economic analysis of maize production was performed after harvest. The input included the values of labor and materials. The labor costs included rotary tillage, sowing, harvesting and field management (weeding, fertilization, etc.). Material costs included maize seed, pesticides, fertilizers and drip irrigation facility. In the PM and BM treatments, the additional labor and material expenses are for the machine film mulching and the material cost of plastic film and biodegradable film, respectively. The output was evaluated based on the economic harvest of grain and straw yields. Total input (*TI*, Yuan ha^{-1}) was calculated as:

$$TI = M_I + L_I \tag{6}$$

where M_I and L_I are material input and labor input, respectively (Yuan ha^{-1}).

Total output (TO, Yuan ha^{-1}) was calculated as:

$$TO = Y \times P_1 + G \times P_2 \quad (7)$$

where G is the yield of dry straw (kg ha^{-1}), and P_1 and P_2 are the price of grain and dry straw of maize, respectively (Yuan kg^{-1}).

Net income (NI, Yuan ha^{-1}) was calculated as:

$$NI = TO - TI \quad (8)$$

2.4. Construction of a Comprehensive Benefits Evaluation System

The AHP qualitatively determined three factors of benefits (i.e., economic, technical and ecological benefits) and their weights, and the GRA quantitatively analyzed the uncertain relationships among factors. A comprehensive evaluation system combining the advantages of AHP and GRA is proposed in this study to analyze the comprehensive benefits of different mulching patterns. The comprehensive benefits evaluation system is shown in Figure 2.

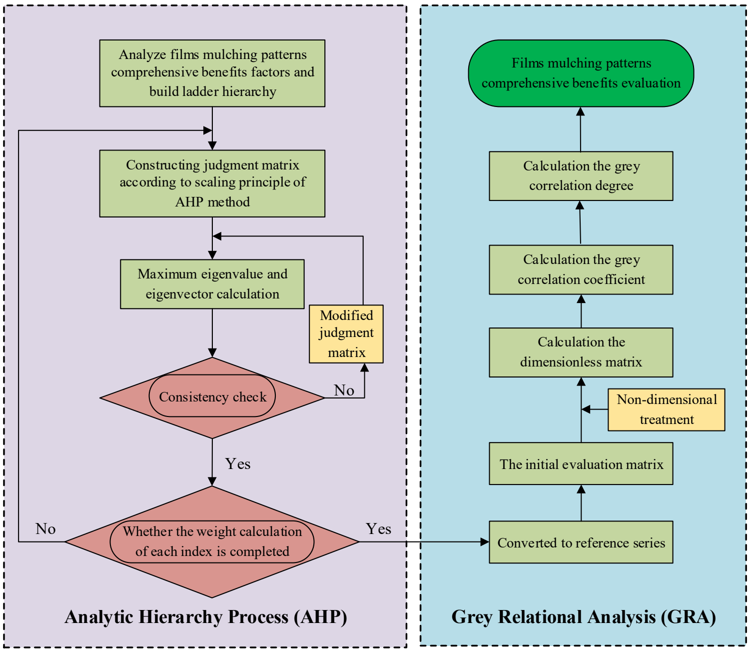

Figure 2. Film mulching patterns comprehensive benefits evaluation system based on AHP-GRE method.

2.4.1. Analytic Hierarchy Process

The process of the AHP method is as follows:

(1) Build the hierarchical structure of the comprehensive evaluation system

The comprehensive evaluation system is divided into three levels from top to bottom. The highest layer is the target layer. The second layer is the criterion layer for evaluating the target layer. The third layer is the specific indicator of the evaluation elements. According to the relationship between the various elements of different mulching patterns, the highest target layer was set as the impact of the different mulching patterns on comprehensive benefits. The criteria layer included the economic benefits, technical benefits and ecological benefits of the different mulching patterns. The indicator layer included the specific indicators that evaluate the economic benefits, technical benefits and ecological benefits, respectively. The comprehensive evaluation system is shown in Figure 3.

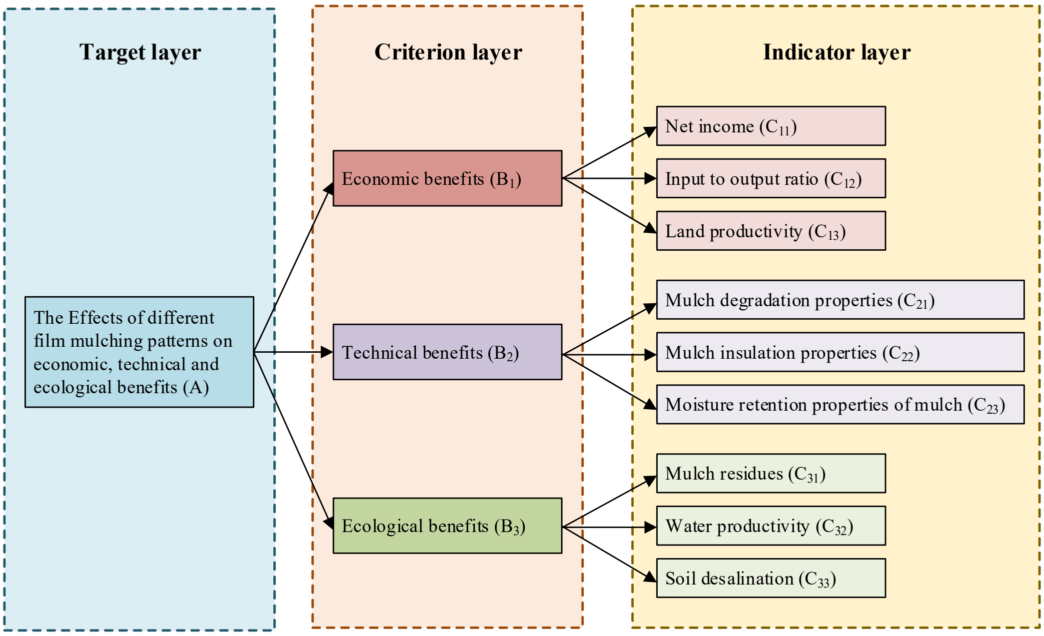

Figure 3. Hierarchical analysis structure.

(2) Construction of a comparative judgment matrix

Judgment matrix is the important degree of each evaluation index in this level for an evaluation element in the previous level. The pairwise comparison judgment matrix was built by the following equation:

$$B = (b_{ij})n \times n = \begin{bmatrix} b_{11} & b_{12} & \cdots & b_{1n} \\ b_{21} & b_{22} & \cdots & b_{2n} \\ \vdots & \vdots & \vdots & \vdots \\ b_{n1} & b_{n2} & \cdots & b_{nn} \end{bmatrix} \tag{9}$$

$$b_{ij} > 0, b_{ji} = \frac{1}{b_{ij}}, b_{ii} = 1 \tag{10}$$

where b_{ij} is the relative important degree of B_i and B_j in the criterion layer relative to the target layer. Its value is determined by the "1–9 Scale Method" (Table 2). N is the number of criterion layer indicators.

Table 2. The 1–9 scaling method and illustration.

Scale Value	Relative Important Degree	Illustration
1	Equally important	Both evaluation elements contribute the same to the goal
3	Slightly important	One evaluation element is slightly more important than another evaluation element
5	Obviously important	One evaluation element is obviously more important than another evaluation element
7	Strongly important	One evaluation element is strongly more important than another evaluation element
9	Extremely important	One evaluation element is extremely more important than another evaluation element
2, 4, 6, 8	Median of two adjacent degrees	Used when compromise is needed

(3) Calculation of normalized weight coefficient (W_i) of the criterion layer

W_i of the criterion layer is calculated as follows:

$$M_i = \prod_{j=1}^{n} b_{ij} \tag{11}$$

$$W_i = \frac{\sqrt[n]{M_i}}{\sum_{i=1}^{n} \sqrt[n]{M_i}} \tag{12}$$

where M_i is the product of each row of the judgment matrix.

2.4.2. Grey Relational Analysis

The process of the GRA method is as follows:

(1) Determination of the reference sequence and comparison sequence

To eliminate the dimension impact of evaluation factor, the sequence should be standardized. The standardization process for comparison sequence is quantified values compared with the average of the standard values. The standardized formulas for comparison sequence and reference sequence are as follows:

$$x_0(k) = \frac{x_0^{(0)}(k)}{\frac{1}{n}\sum_{i=1}^{n} x_i^{(0)}(k)} \tag{13}$$

$$x_i(k) = \frac{x_i^{(0)}(k)}{\frac{1}{n}\sum_{i=1}^{n} x_i^{(0)}(k)} \tag{14}$$

where i = 1, 2, . . . , n; k = 1, 2, . . . , m; $x_0(k)$ represents standard values of kth evaluation factor in evaluation samples; $x_i(k)$ represents standard values of kth evaluation factor in level i evaluation standard; and $x_0^{(0)}(k)$ (k = 1, 2, . . . , m) is the comparison sequence. The subscript 0 represents samples to be evaluated, and k represents the evaluation factor. $x_i^{(0)}(k)$ (i = 1, 2, . . . , n; k = 1, 2, . . . , m) is the reference sequence.

(2) Calculation of grey correlation coefficient

The grey correlation coefficient (ξ) is as follows:

$$\xi_i(k) = \frac{\min_i \min_k \left| x_0^{(0)}(k) - x_i^{(0)}(k) \right| + \rho \max_i \max_k \left| x_0^{(0)}(k) - x_i^{(0)}(k) \right|}{\left| x_0^{(0)}(k) - x_i^{(0)}(k) \right| + \rho \max_i \max_k \left| x_0^{(0)}(k) - x_i^{(0)}(k) \right|} \tag{15}$$

where ρ is the resolution coefficient; generally, the value takes 0.5 [36].

(3) Calculation of grey weighted correlation.

For some sequence, when the various factors have the different importance, according to the role of the various indices, different weights were given. The weighted correlation of the sequence being evaluated is as follows:

$$R_k = \sum_{k=1}^{n} w_k \times \xi_i(k) \tag{16}$$

where R_k is the grey weighted correlation; w_k is the weight determined by AHP.

2.5. Statistical Analysis

One-way analysis of variance (ANOVA) using SPSS 20.0 software (IBM, SPSS Statistics, New York, NY, USA) was performed to test the differences among the treatments. Multiple comparisons were made using Tukey's test at the 5% level (i.e., indicating significance at $p < 0.05$). The figures were drawn by OriginPro 2022 (OriginLab Software, Northampton, MA, USA).

3. Results

3.1. Climatic Conditions

The daily air temperatures, rainfall distributions and full irrigation amount in 2020 and 2021 are shown in Figure 4. Throughout the maize season of 2020, the average temperature was 19.5 °C, and the range in high and low temperatures was 13~36 and 1~20 °C, respectively. Similarly, the average temperature was 19.9 °C, high and low temperatures ranged over 16~39 and 3~21 °C during 2021, respectively. Total precipitation over the whole growing period amounted to 131.8 mm in 2020 and 154.6 mm in 2021. Compared with 2020, the rainfall amount increased by 12.8 mm in 2021, and was mainly distributed in the later stages of maize growth. The total irrigation amounts under full irrigation treatment were 344.9 for 2020 and 357.7 mm for 2021 during the maize growing season, respectively.

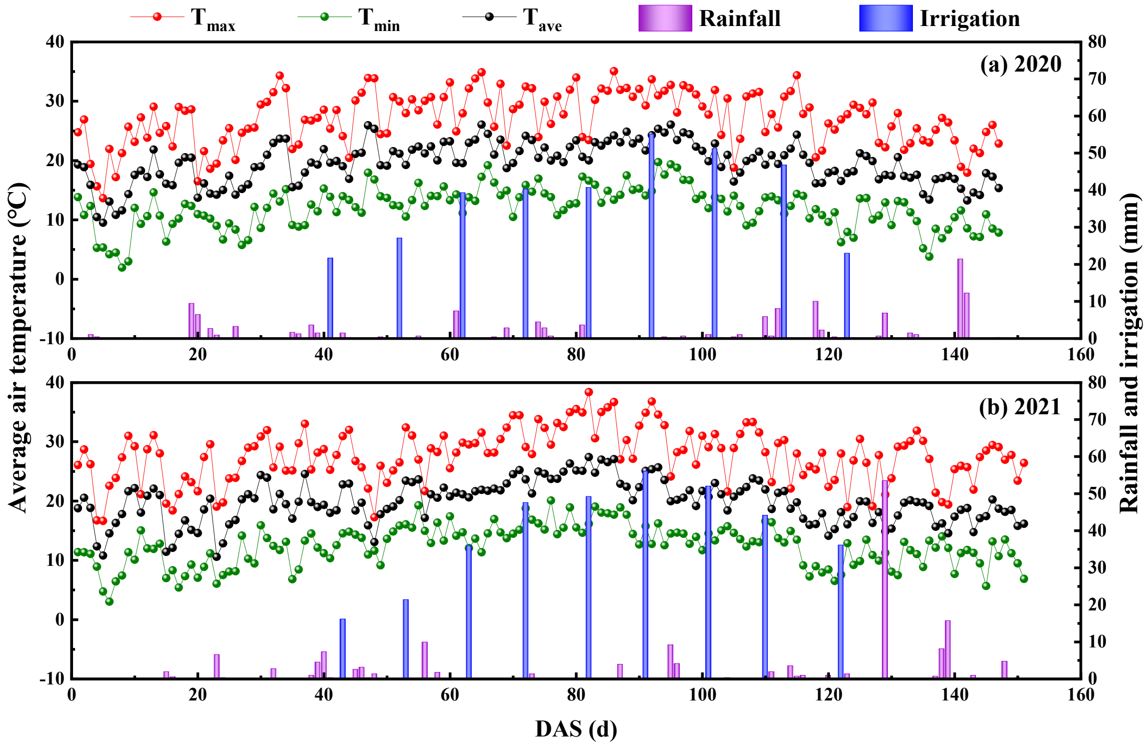

Figure 4. Daily rainfall amount, full irrigation amount and air temperature in 2020 (**a**) and 2021 (**b**).

3.2. Film Degradation Process and the Film Weight Loss Rate

Table 3 shows the different degradation performances for BM and PM treatments. Biodegradable film under FI, MI and LI treatments already showed signs of degradation at 45 DAS. At 90 DAS, the film showed 2~2.5 cm cracks under BMFI treatment, and 25% of the film showed fine cracks under BMMI and BMLI treatments in the fields. At 135 DAS (pre-harvest of maize), the films broke into small fragments under BMFI and BMMI treatments, and no larger remains were on the soil surface, which indicated BMFI and BMMI entered film degradation stage IV. On the whole, similar trends of the film degradation were found in 2020, as those in 2021.

Table 3. The degradation process of film under three irrigation strategies for the maize growing seasons in 2020 and 2021.

Treatment		**Days after Sowing (d)**							
		30	**45**	**60**	**75**	**90**	**105**	**120**	**135**
2020~2021									
PM	FI	Null	Null	Null	Null	Null	Null	I	I
	MI	Null	Null	Null	Null	Null	I	I	I
	LII	Null	Null	Null	Null	Null	Null	Null	I
BM	FI	Null	I	II	II	III	III	III	IV
	MI	Null	I	II	II	II	II	III	IV
	LI	Null	I	II	II	II	II	III	III
2021~2022									
PM	FI	Null	Null	Null	Null	Null	I	I	I
	MI	Null	Null	Null	Null	Null	Null	I	I
	LI	Null	Null	Null	Null	Null	Null	I	I
BM	FI	Null	I	II	II	III	III	III	IV
	MI	Null	I	II	II	II	III	III	IV
	LI	Null	I	I	II	II	II	III	III

The sowing date was 1 May and 3 May in the 2020 and 2021 growing seasons, respectively (annual film mulching three days earlier than sowing). Stage I indicates that after the induction period, the film had begun to crack; Stage II indicates that 25% of the film appeared to show tiny cracks; Stage III indicates that the cracks in the film were 2~2.5 cm in width, and the number of cracks increased; Stage IV indicates that film breaks into small fragments, no large pieces of film, and the cracks were uniform and reticular; Stage V indicates that almost no residual film pieces existed on the soil surface and the film was degraded into fragments smaller than 4×4 cm^2 (null indicates the film is practically intact).

Figure 5 summarized the film weight loss rate under different irrigation strategies (FI, MI and LI treatments) after maize harvest, which were 38.8%, 36.1% and 32.9% in 2020, respectively, and 41.3%, 37.1% and 35.1% in 2021, respectively. Compared with LI treatment, the BM weight loss rate under FI treatment increased by 6.1% and was significantly different ($p < 0.05$). The PM film weight loss rate was 12.0%, and no significant difference among treatments was observed in 2020 and 2021. The weight loss rate may be caused by accidental wear and tear due to mechanical pulling and human activity.

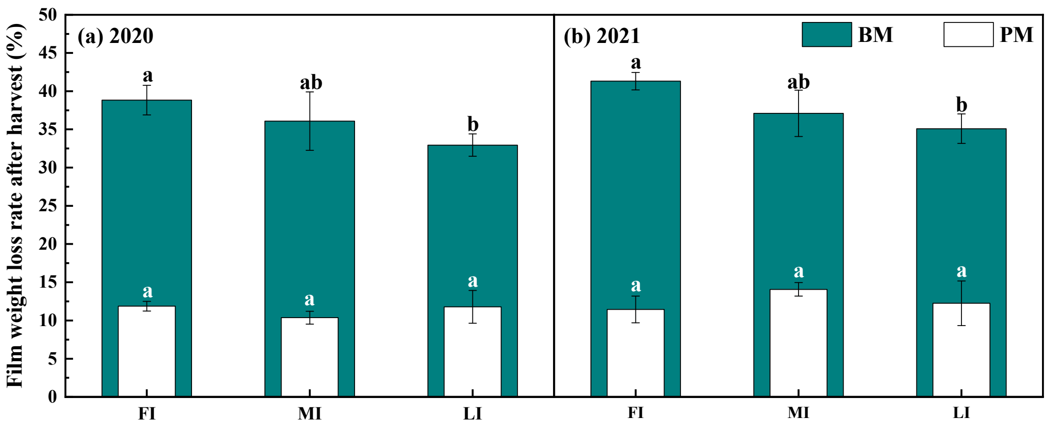

Figure 5. The weight loss rates under BM of different irrigation strategies (FI, MI and LI treatments) after maize harvest in 2020 (**a**) and 2021 (**b**). Different superscripted letters (a and b) indicate significant differences between treatments in each year at $p < 0.05$.

3.3. Soil Water Storage

SWS to the soil depth of 1 m varied significantly in 2020 and 2021 (Table 4). At 34 DAS (2020) and 29 DAS (2021), compared with pre-sowing SWS, the SWS in the NM, PM and BM treatments were decreased by 42.4, 23.9 and 22.7 mm in 2020 and decreased by 39.1, 22.0 and 27.9 mm in 2021, respectively. The SWS of all treatments increased after sowing (with irrigation to ensure seedling emergence) and then decreased over time during 0~62 DAS.

SWS was higher in FI than MI and LI during 62 to 123 DAS in 2020 (62 to 121 DAS in 2021), but there were significant differences only during 90 and 121 DAS in 2021 ($p < 0.05$). Based on the NM, PM and BM treatments, the SWS at 136 DAS decreased by 2.4, 2.6 and 2.8 mm compared with 123 DAS for 2020, respectively. In addition, the SWS at 141 DAS increased by 17.9, 23.1 and 14.7 mm compared with 121 DAS for 2021, respectively, which may be due to strong rainfall (53.4 mm) at 129 DAS in 2021.

Table 4. Soil water storage (SWS) evolution in the 0~100 cm soil layer in 2020 and 2021.

Treatment		2020 (2021) Days after Sowing (d)					
		0 (0)	34 (29)	62 (62)	92 (90)	123 (121)	136 (141)
2020–2021							
NM	FI	163.9 ± 7.5 a	206.6 ± 11.2 a	186.8 ± 12.3 a	182.1 ± 10.4 a	185.0 ± 17.1 a	191.5 ± 16.4 a
	MI	125.1 ± 6.5 a	169.6 ± 23.1 a	157.6 ± 21.7 a	131.8 ± 36.6 a	136.4 ± 29.6 a	134.0 ± 23.2 a
	LI	136.6 ± 15.9 a	176.7 ± 21.6 a	155.0 ± 12.2 a	144.4 ± 15.1 a	140.4 ± 17.0 a	139.2 ± 14.8 a
PM	FI	150.2 ± 20.7 a	178.1 ± 16.7 a	155.9 ± 7.5 a	144.3 ± 12.5 a	170.0 ± 48.1 a	177.4 ± 53.3 a
	MI	138.9 ± 8.5 a	148.8 ± 24.6 a	145.8 ± 4.9 a	131.6 ± 1.9 a	138.4 ± 8.4 a	133.4 ± 4.6 a
	LI	147.6 ± 40.6 a	181.7 ± 36.2 a	152.9 ± 28.8 a	143.1 ± 14.8 a	152.3 ± 12.1 a	152.2 ± 17.8 a
BM	FI	155.0 ± 20.3 a	179.2 ± 22.1 a	174.9 ± 14.0 a	166.4 ± 19.2 a	206.5 ± 32.9 a	200.2 ± 26.0 a
	MI	132.3 ± 7.9 a	152.9 ± 32.5 a	142.5 ± 21.1 a	144.9 ± 36.8 a	146.0 ± 24.1 a	148.5 ± 18.7 a
	LI	143.5 ± 19.2 a	166.8 ± 14.1 a	144.0 ± 16.9 a	140.2 ± 14.6 a	136.9 ± 7.6 a	132.4 ± 7.4 a
2021–2022							
NM	FI	175.1 ± 9.8 ab	216.2 ± 6.4 a	192.2 ± 1.2 a	167.7 ± 9.6 a	172.5 ± 12.5 a	183.0 ± 14.4 a
	MI	137.9 ± 16.2 ab	163.3 ± 40.1 a	147.2 ± 19.5 a	128.9 ± 15.4 b	128.8 ± 12.7 b	146.9 ± 12.6 a
	LI	145.0 ± 16.4 ab	195.7 ± 12.3 a	176.9 ± 22.9 a	139.5 ± 18.2 ab	135.5 ± 13.5 ab	160.6 ± 13.6 a
PM	FI	175.7 ± 22.2 ab	178.3 ± 16.5 a	159.5 ± 17.9 a	130.5 ± 3.2 ab	136.9 ± 3.7 ab	156.0 ± 17.8 a
	MI	143.6 ± 7.4 ab	168.5 ± 10.7 a	150.5 ± 3.6 a	124.3 ± 6.2 b	121.3 ± 7.6 b	142.7 ± 6.0 a
	LI	158.8 ± 17.5 ab	197.3 ± 24.6 a	157.3 ± 18.5 a	151.1 ± 14.7 ab	139.3 ± 14.8 ab	162.2 ± 19.6 a
BM	FI	180.2 ± 22.2 a	221.6 ± 25.9 a	188.2 ± 33.7 a	148.4 ± 13.3 ab	156.5 ± 21.9 ab	179.8 ± 35.5 a
	MI	155.4 ± 9.1 ab	169.2 ± 17.3 a	133.1 ± 24.8 a	122.7 ± 18.8 b	118.0 ± 26.1 b	132.1 ± 28.0 a
	LI	134.5 ± 9.6 b	163.0 ± 18.7 a	162.9 ± 25.7 a	135.1 ± 9.1 ab	127.6 ± 8.6 b	134.4 ± 9.8 a

Note. Different letters (a and b) indicate significant differences among SWS of different treatments at $p < 0.05$.

Figure 6 shows the relative ET (ET_r, i.e., the ratio of ET at one specific period to the total ET during the crop growth period). From sowing to the first irrigation (41 DAS in 2020 and 43 DAS in 2021), the ET_r under BM treatment was higher than under PM and NM treatments, with an average increase of 4.9% and 0.7% in 2020 and 2.1% and 0.6% in 2021, respectively. During 34 to 62 DAS in 2020 (62 to 121 DAS in 2021), the ET_r in the NM treatment was 2.1% (1.4%) higher than in PM and 2.4% (1.0%) higher than in the BM treatment. During 124 to 136 DAS in 2020 (122 to 141 DAS in 2021), the ET_r decreased gradually in all treatments without significant difference.

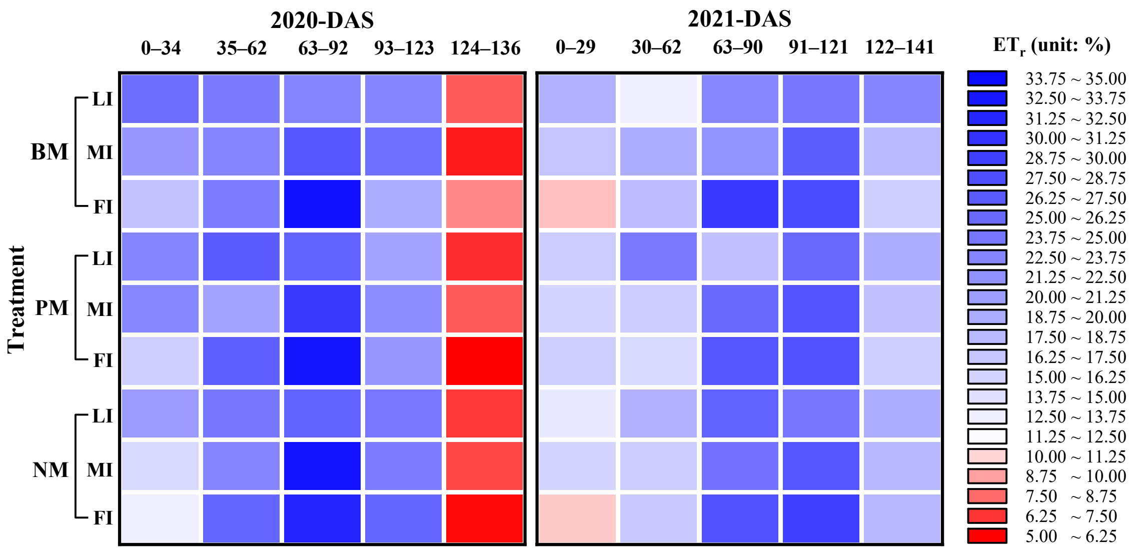

Figure 6. ET_r of each film degradation stage under different treatments in 2020 and 2021.

3.4. Soil Temperature

The variations in daily average T_s of 0~20 cm soil depth under different film mulching treatments are shown in Figure 7. The daily evolution of T_s was similar between the BM and PM treatments, and T_s were all significantly higher than in the NM treatment ($p < 0.05$). T_{s_BM} (i.e., T_s in BM treatment) was 0.9 and 1.0 °C higher than T_{s_NM} (i.e., T_s in NM treatment) and 0.6 and 0.4 °C lower than T_{s_PM} (i.e., T_s in PM treatment) over the two growing seasons of 2020 and 2021, respectively.

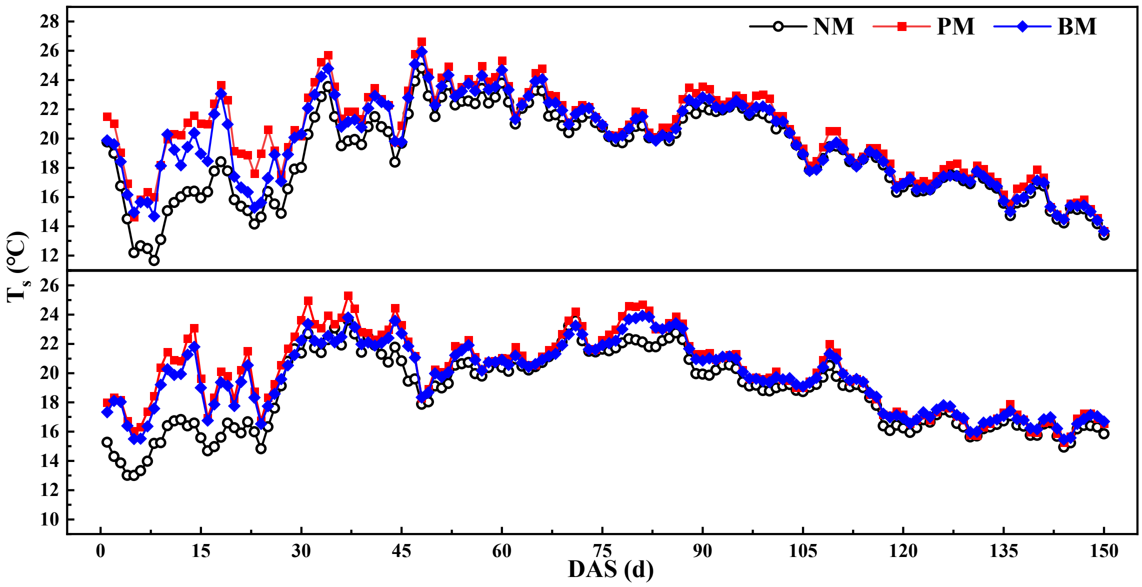

Figure 7. Evolution of daily average soil temperature of 0~20 cm depth among various treatments in 2020 and 2021. NM, PM and BM represent non-mulching, transparent polyethylene plastic film mulching and biodegradable film mulching, respectively.

Figure 8 shows the accumulation of T_{s_PM}–T_{s_NM} and T_{s_BM}–$Ts_{\_NM}$ under different film degradation stages in 2020 and 2021. The accumulation of T_{s_PM}–T_{s_NM} and T_{s_BM}–T_{s_NM} during 0 to 30 DAS were significantly higher than 31 to 60, 61 to 90, 91 to 120 and 121 to 150 DAS over two growing seasons, respectively. At various degradation stages (i.e., 0 to 30, 31 to 60, 61 to 90, 91 to 120 and 121 to 150 DAS), the accumulation of T_{s_PM}–T_{s_NM} was generally higher than T_{s_BM}–T_{s_NM}, with an increase of 63.7, 12.5, 11.0, 6.7 and 10.7 °C in 2020 and 22.7, 18.1, 12.9, 3.5 and -1.7 °C in 2021, respectively. There were significant differences only in the initial maize growth stage (0 to 30 DAS) between the accumulation of T_{s_PM}–T_{s_NM} and T_{s_BM}–T_{s_NM} ($p < 0.05$).

Figure 9 compares the soil effectively accumulated temperature (SEAT) under the NM, PM and BM treatments (Figure 9a,c) and the air effectively accumulated temperature (AEAT) (Figure 9b) for 2020 and 2021. The AEATs of the two growing seasons were 1692.9 and 1790.7 °C, respectively. The PM treatment had the highest SEAT, followed by BM and NM. The SEAT under BM treatment was not significantly different from the PM and NM treatments, increasing by 150.3 °C (8.5%) compared with the NM treatment and decreasing by 72.8 °C (4.1%) compared with the PM treatment. However, the SEAT under the PM treatment was 223.3 and 223.1 °C higher than in the NM treatment in 2020 and 2021, respectively, which was significantly different ($p < 0.05$).

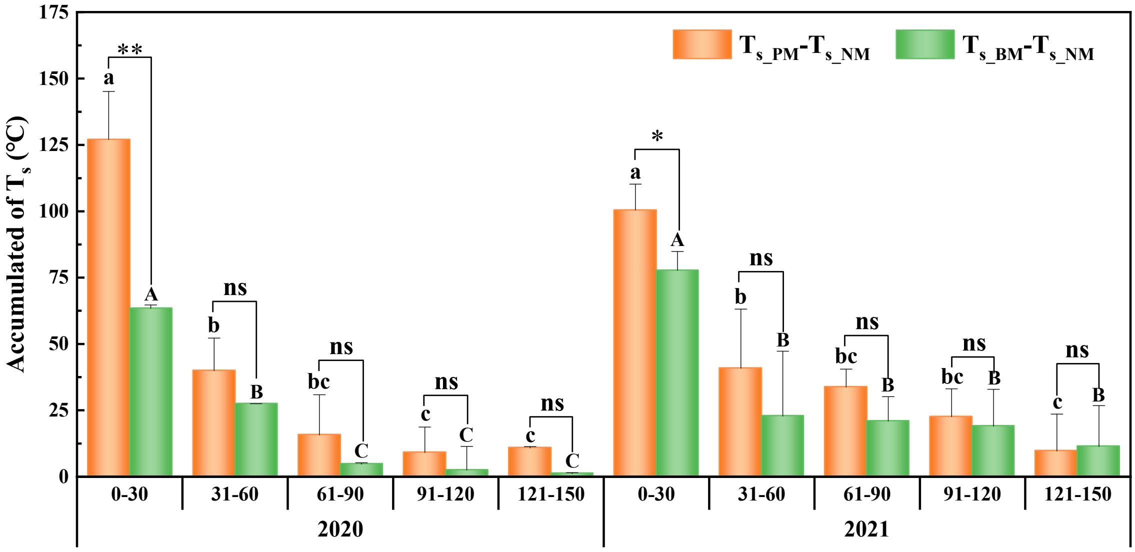

Figure 8. Accumulation of T_{s_PM}−T_{s_NM} (in yellow) and T_{s_BM}−T_{s_NM} (in green) during crop growth period in 2020 and 2021. Bars stand for standard error. Different lowercase (capital) letters above the bars indicate significant differences among T_{s_PM}−T_{s_NM} (T_{s_BM}−T_{s_NM}) of degradation film degradation stages at $p < 0.05$. * (**) represents the significant difference between T_{s_PM}−T_{s_NM} and T_{s_BM}−T_{s_NM} at the same degradation stages of degradation film at the level $p < 0.05$ ($p < 0.01$). "ns" means no significant difference. NM, PM and BM represent non-mulching, transparent polyethylene plastic film mulching and biodegradable film mulching, respectively.

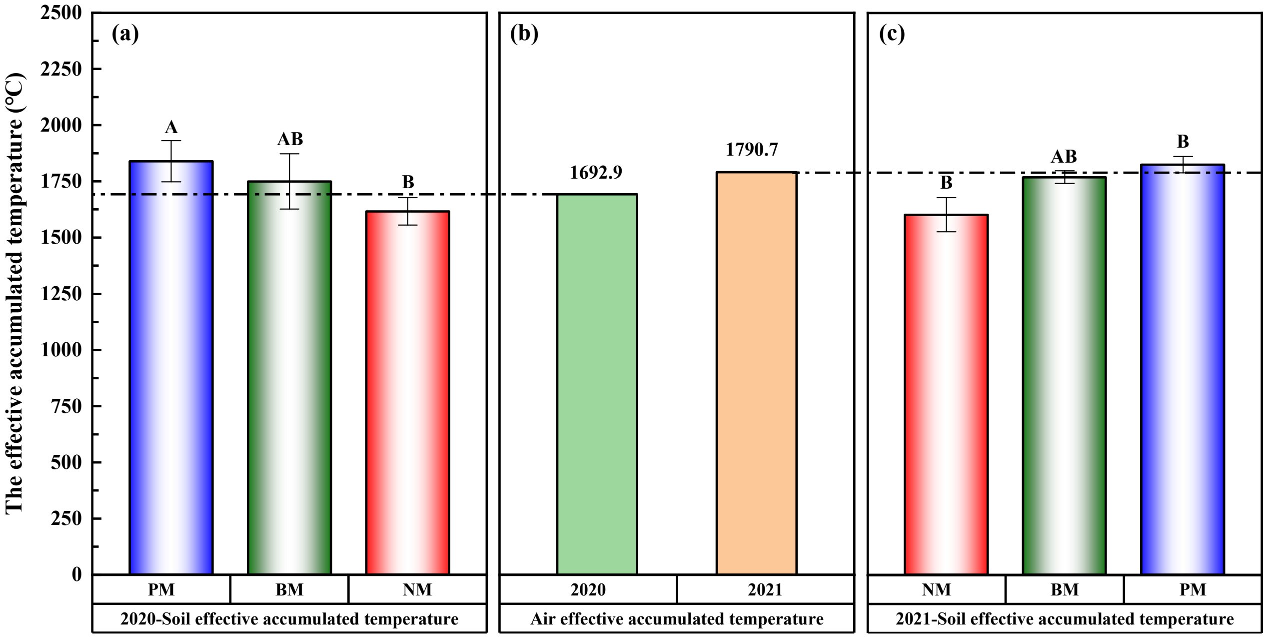

Figure 9. Soil effective accumulated temperature (SEAT) under NM, PM and BM treatments for 2020 (**a**) and 2021 (**c**). Air effective accumulated temperature (AEAT) for 2020 and 2021 (**b**). Bars stand for standard error. Any two bars in the same figure and year with different capital letters above the bars are significantly different at $p < 0.05$. NM, PM and BM represent non-mulching, transparent polyethylene plastic film mulching and biodegradable film mulching, respectively.

3.5. Maize Growth

3.5.1. Growth Stages

The DAS for maize reaching the different growth stages under different film mulching treatments are shown in Figure 10. The BM and PM treatments significantly increased

T_s in the early growth period and shortened the time to harvest. The initial stage in the BM treatment was 3 and 6 days longer than in the PM treatment and 9 and 7 days shorter than those of the NM treatment in 2020 and 2021, respectively. After maize entered the development stages of growth, the growth stage progress under BM and PM treatments was similar. Overall, the DAS of mature under BM and PM treatments was 136 and 141 days, shortened by 11 and 10 days compared with NM treatment in 2020 and 2021, respectively.

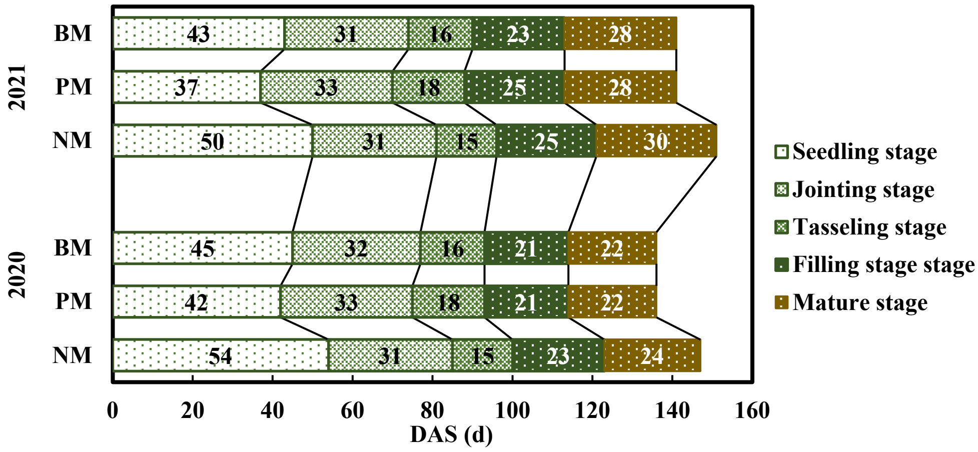

Figure 10. Growth stages of maize under different film mulching patterns.

3.5.2. Yield and WP

The yield components (i.e., spike length, ear diameter, 100-kernel weight), grain yield and WP of maize were significantly ($p < 0.05$) affected by mulching patterns and irrigation strategies (Table 5). In 2020 and 2021, the grain yield of maize in the BMFI treatment reached 18.1 and 14.9 t ha^{-1}, which increased by 5.8% and 12.4% compared with those of the NMFI treatment. When compared with the PMFI treatment, the grain yield of maize decreased by 1.7% in 2020 and increased by 0.6% in 2021. The WP of the BMFI treatment was the highest, reaching 4.1 and 2.9 kg m^{-3} in 2020 and 2021, with an increase of 12.5% and 10.2% over the NMFI treatment and 3.3% and 2.6% over the PMFI treatment, respectively. Though there was no significant difference in grain yield and WP under different film mulching patterns with the same amount of irrigation, the decrease in the irrigation amount significantly reduced grain yield and increased WP ($p < 0.05$). Under the same film mulching pattern, compared with FI treatment, grain yield in MI and LI treatments decreased by 10.4~12.2% and 30.0~34.6% in 2020 and 20.7~25.4% and 23.2~29.6% in 2021, respectively; the WP in the MI and LI treatments increased by 2.1~15.4% and 8.6~17.1% in 2020 and 2.7~6.1% and 22.0~33.8% in 2021, respectively.

3.6. Benefits Assessment

3.6.1. Economic Benefits

As shown in Figure 11, the economic parameters of maize under the nine treatments were evaluated in 2020 and 2021. In general, the net income for the NM, PM and BM treatments were CNY 10,041~22,060, CNY 11,853~22,060 and CNY 9172~18,412 ha^{-1} in 2020 and CNY 5578~14308, CNY 6880~14,834 and CNY 4808~13,352 ha^{-1} in 2021, respectively. During the two growth seasons, the highest value was obtained in the PMFI treatment, and the lowest value was recorded in the BMLI treatment, and the amount of irrigation water showed a significant effect on the net income of each treatment ($p < 0.05$). The total input cost of the BM treatment is the highest among all treatments, which was CNY 2450 ha^{-1} and CNY 1080 ha^{-1} higher than the NM and PM treatments, respectively. The BM treatment average total output increased by CNY 1690 ha^{-1} compared with the NM treatment and decreased by CNY 562 ha^{-1} compared with the PM treatment, respectively.

Table 5. Yield components, grain yield and WP of maize under all treatments in 2020 and 2021.

Treatment		Spike Length (cm)	Ear Diameter (mm)	100-Kernel Weight (g)	Grain Yield ($kg{\cdot}ha^{-1}$)	WP ($kg{\cdot}m^{-3}$)
2020–2021						
NM	FI	21.23 a	53.42 a	37.89 c	17.15 ab	3.68 b
	MI	20.96 ab	48.99 bc	37.68 b	15.06 bc	4.24 ab
	LI	19.67 bcd	48.68 bc	40.41 b	11.21 d	4.21 ab
PM	FI	19.87 abcd	49.26 b	44.15 a	18.46 a	4.00 ab
	MI	19.12 cd	48.09 bc	42.81 ab	16.32 ab	4.09 ab
	LI	17.62 ef	45.81 d	41.63 ab	12.93 cd	4.69 a
BM	FI	20.02 abc	49.75 b	43.14 ab	18.14 a	4.13 ab
	MI	18.57 de	48.62 bc	42.47 ab	16.26 b	4.47 ab
	LI	16.93 f	44.61 d	40.85 b	12.23 d	4.49 ab
2021–2022						
NM	FI	18.12 a	47.62 ab	43.95 c	13.26 ab	2.59 d
	MI	16.62 ab	46.78 abc	43.35 c	10.51 cd	2.66 cd
	LI	14.67 bc	45.25 bc	43.39 bc	9.33 d	3.16 bc
PM	FI	18.40 abc	48.97 a	45.38 a	14.81 a	2.79 cd
	MI	16.76 cd	44.05 c	45.59 ab	11.72 bc	2.96 cd
	LI	15.39 de	46.58 abc	47.36 ab	11.37 bcd	3.73 a
BM	FI	18.52 abc	48.89 a	47.62 ab	14.90 a	2.86 cd
	MI	16.23 cd	45.59 bc	45.34 ab	11.11 bcd	2.71 cd
	LI	15.24 e	45.56 bc	45.03 bc	10.63 dc	3.50 ab

Note: Different letters (a, b, c and d) indicate significant differences among yield components, grain yield and WP of maize under different treatments at $p < 0.05$.

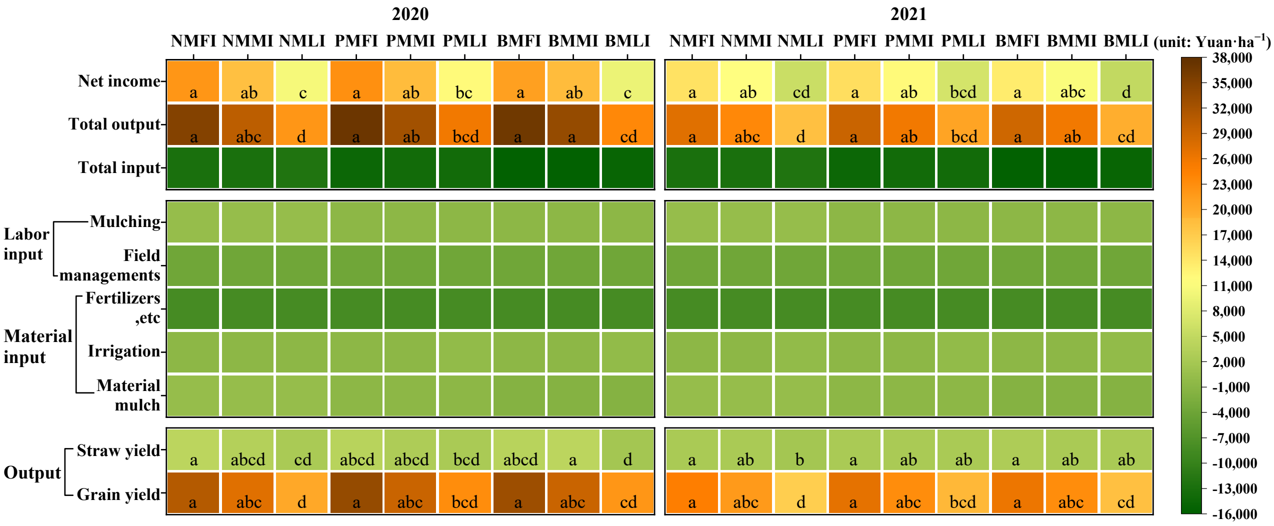

Figure 11. Economic benefits in response to different treatments in 2020 and 2021. Different letters (a, b, c and d) within a line indicate significant difference among treatments within each growth season at $p < 0.05$.

3.6.2. Comprehensive Benefits under Different Film Mulching Patterns

According to the comprehensive evaluation system established in Section 2.4 for different mulching patterns under the same irrigation strategy (i.e., FI treatment), indicators including net income (C_{11}), mulch degradation properties (C_{21}), mulch residues (C_{31}), etc., are quantified. The total weight matrix is A = (0.571, 0.143, 0.286, 0.600, 0.200, 0.200, 0.625, 0.239, 0.136) (Table 6). After the consistency check, the CRs (test coefficient) of each judgment matrix were 0.026, 0 and 0.018 (less than 0.10), respectively. Each judgment matrix shows satisfactory consistency, indicating there was no logical confusion in the priority of indicators. Only in terms of economic benefits did the PM treatment perform the best, followed by the NM treatment (Figure 12). The NM treatment had the highest benefit based on technical or ecological benefits alone, followed by the BM treatment. On the whole, the combined benefits of considering economic, technical and ecological benefits under each film mulching pattern were ranked as NM > BM > PM in the arid region of northwest China.

Table 6. Correlation coefficients and weights for each indicator.

Criterion Layer	Weights	Indicator Layer	Weights	Correlation Coefficients		
				NM	PM	BM
Economic benefits	0.297	Net income	0.571	0.982	1.000	0.955
Technical benefits	0.163	Input to output ration	0.143	1.000	0.981	0.936
Ecological benefits	0.540	Land productivity	0.286	0.963	1.000	0.991
		Mulch degradation properties	0.600	1.000	0.468	0.595
		Mulch insulation properties	0.200	0.483	1.000	0.646
		Moisture retention properties of mulch	0.200	0.669	0.555	1.000
		Mulch residues	0.625	1.000	0.540	0.575
		Water productivity	0.239	0.949	0.987	1.000
		Soil desalination	0.136	0.423	0.333	1.000

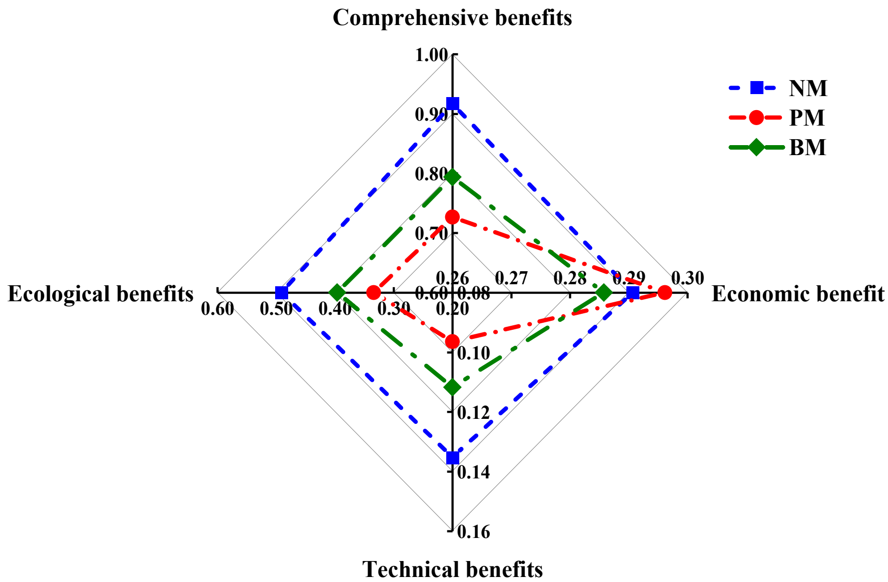

Figure 12. Economic, technical, ecological and comprehensive benefits of different film mulching patterns.

4. Discussion

4.1. Effect of Irrigation Strategies on Degradation of Biodegradable Film

The biodegradable film degradation rate mainly depends on the degradation materials and environmental conditions [8,53]. Differences in the natural environment of different regions such as soil moisture, sunlight, air temperature extremes and wind speed may cause differences in the degradation time and degree [29,54,55]. In this study, the same type of biodegradable film was used in the 2020 and 2021 experiments. Both years show that the degradation rate of the biodegradable film was the fastest under the FI treatment and the slowest under the LI treatment. Furthermore, the amount of irrigation also had a significant effect ($p < 0.05$) on the biodegradable film′s weight loss rate after maize harvest, with the highest film weight loss rate of 38.8% under the FI treatment. These results were similar to previous research findings [56–60]. In a hybrid maize experiment, Zhang et al. [28] found that the biodegradable film degradation rate in 2017, with lower soil moisture, was slightly lower than in 2016 with relatively higher soil moisture. These studies further confirmed that the large number of rapidly growing microorganisms induced by the wetter soil might be responsible for the accelerated rate of film degradation; that is, relatively high soil water content might accelerate the degradation of biodegradable film. However, premature cracking failure of the biodegradable film may reduce the benefit of film mulching for enhancing soil temperature and conserving soil water [22]. Yin et al. [48] demonstrated that the optimum degradation induction period (the time to enter biodegradation stage I) for BM was about 50 d, which performed better than a 20 d induction period in arid and semi-arid regions. In terms of this study, although BM degradation was accelerated under FI, with its induction period reduced to 45 d, it was close to the optimum degradation rate and would be acceptable. Therefore, in this study, BM under FI treatment not only increased the temperature of the early crop growth stage, but it also showed more efficient use of rainfall with more degradation cracks than those under LI treatment, as confirmed by Chen et al. [61].

4.2. Effects of Mulching and Irrigation on the Soil Temperature and Soil Water Storage

Low temperature is one of the main factors restricting crop germination [62,63]. Generally, the effects of BM and PM treatments on increasing T_s have been widely documented [26,28,64]. In this study, the differences in the accumulation of $T_{s\_PM}–T_{s\_NM}$ and $T_{s\_BM}–T_{s\_NM}$ under different film degradation stages during the crop growth period were also quantified in 2020 and 2021 (Figure 8). These results indicated that the PM and BM treatments significantly increased T_s only during the early stages of crop, and T_{s_BM} behaved in a similar way to T_{s_NM} after film degradation ($p < 0.05$) (Figures 7 and 8), which was consistent with those results by Gu et al. [65]. Previous studies have shown that SEAT was tightly linked with the process of crop growth and development [56,66]. A similar result was found in the current study: The SEAT under BM treatment increased by 8.5% compared with NM treatment and decreased by 4.1% compared with PM treatment (Figure 9). Therefore, a suitable T_s could accelerate plant growth, maintain root activity and increase crop yield [48,67].

The variations in the SWS during the growing season depended on the rainfall, soil evaporation and crop consumption for growth [68]. Many studies have demonstrated that both PM and BM can greatly maintain the SWS by reducing soil evaporation, especially during the early crop stages [4,69]. In this experiment, during film degradation stages I~III (from 0 to 90 DAS), the ETs of the PM and BM treatments were higher than the NM treatment under the same irrigation strategy. Generally, we assume that film mulching restricted the soil evaporation and should show lower ET in the earlier crop stage. However, film mulching advanced crop development by enhancing soil temperature and tended to boost leaf area and canopy coverage of maize, thus increasing crop transpiration (T) and resulting in a higher ET under mulched conditions during film degradation stages I~III. This result agrees with observations previously reported by Gong et al. [70] and Zhao et al. [4]. During film degradation stages III~IV (from 90 DAS to harvest), the ET of the NM treatment was significantly higher than the PM and BM treatments under same irrigation strategy ($p < 0.05$), and there was no significant difference between the ETs of the PM and BM treatments. This result is expected because maize with film mulching accelerated senescence at film degradation stages III~IV (i.e., the middle and later maize growth stages). The maize canopy of NM tended to have higher LAI than PM and BM (Figure 13); thus, the transpiration of NM in this period was higher. On the whole, in this study, there was a decrease in ET under the PM and BM treatments during the two maize-growing seasons, which was consistent with that reported in the literature [71–74].

4.3. Effects of Mulching and Irrigation on the Crop Growth and WP

Previous studies have that mulching treatments significantly increased yield since film mulching reduced soil evaporation and improved soil hydrothermal conditions [2,75,76]. This study confirmed the previous reports. In addition, although the grain yield of maize was usually lower for BM than PM treatment, there was no significant difference between these treatments in this study (Table 5). This result was consistent with the previous studies on various crops, including summer maize [19], wheat [20], tomato [77], zucchini [78], strawberry [79], cotton [80] and peanut [27]. It is worth noting that the difference in grain yield between FI and LI treatments reduced after mulching over two growth seasons

(Table 5), which indicated that film mulching could be particularly beneficial to yield formation in cold areas with water shortages. Most of the studies elaborated that exposure to heat stress reduced pollen number and viability, reduced silk growth and ovary growth and weakened silk. Thus, the kernel number was significantly reduced [81,82]. In this study, the local air temperature might be higher than the appropriate growth temperature at the filling stage of maize. During the same period (90 DAS), the number of cracks in the degraded film increased and reached degradation level III; the BM treatment could avoid the negative effects of high temperatures and make more efficient use of rainfall compared with PM. Furthermore, DI generally increased the ratio of root to shoot, which was beneficial for improving water absorption and enhancing soil nutrient uptake [25]. Therefore, the combination of biodegradable film and deficit irrigation could not only be beneficial to grain yield formation but also to reducing irrigation and improving water productivity. Meanwhile it is more friendly to the soil environment [2,55]. Water is the main limiting factor for crop growth in dryland farming areas, and PM is widely used to improve WP compared with NM [5]. In the present study, PM and BM increased WP by 7.51–18.0% and 2.0–12.5% compared with NM, respectively, and these results were similar to those from earlier studies [48,49]. The main reason was that film mulching can effectively restrict soil water loss via soil evaporation and increase canopy transpiration, biomass accumulation and, ultimately, grain yield [56]. Lin et al. further confirmed that PM may have little impact on the sum of ET because it increased transpiration and reduced evaporation, and it is beneficial to enhancing water productivity with PM [5]. Therefore, in the long run, the combination of biodegradable film and deficit irrigation may act as a promising agricultural management system to improve maize yield, WP and simultaneously reduce soil environmental risks in arid and semi-arid regions in China.

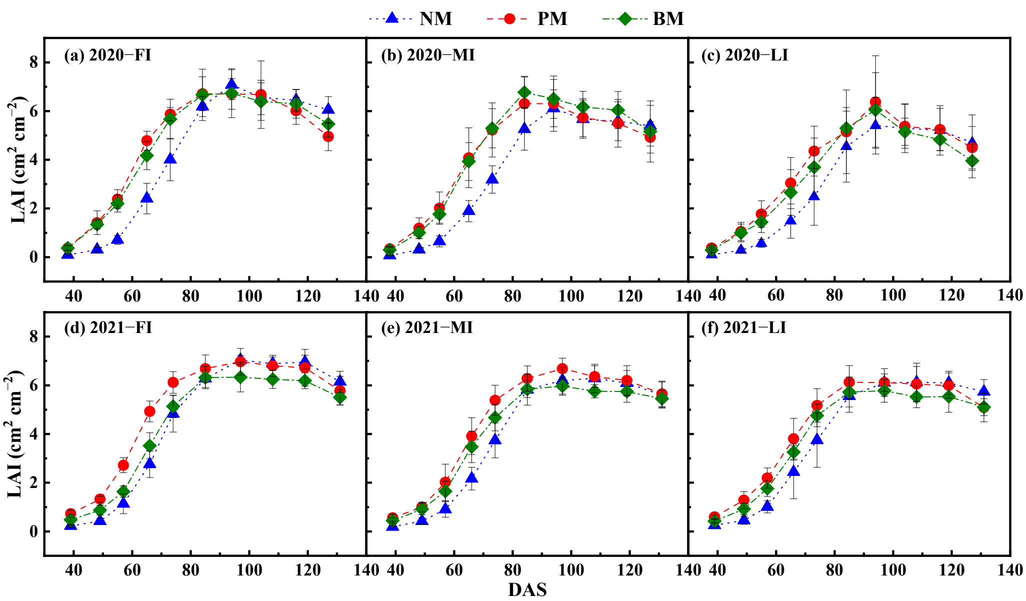

Figure 13. Evolution of maize leaf area index (LAI) under different mulching treatments for three irrigation levels, FI (**a**), MI (**b**) and LI (**c**) in 2020 and FI (**d**), MI (**e**) and LI (**f**) in 2021, respectively. NM, PM and BM represent non−mulching, transparent polyethylene plastic film mulching and biodegradable film mulching, respectively.

4.4. Comprehensive Benefits Evaluation of Different Film Mulching Patterns Based on AHP-GRE Methods

In this study, net income was lower for BM treatment compared with PM and NM treatments over two growth seasons (Figure 11). This finding agrees with observations previously reported by Sun et al. [27]. There are two possible reasons for this. First, the price of biodegradable films is higher than transparent PE films. Second, the BM and PM treatments had additional labor input costs for the film sheet installation [28]. Therefore, compared with NM and PM treatments, the material cost of BM treatment increased by 19.1% and 11.4%, respectively. In addition, the labor cost of film sheet installation increased by 20.2% compared with the NM treatment. In addition, according to the local situation, the total output included straw yield and grain yield in this study. Although the BM treatment′s total output was much larger than the NM treatment′s, its material cost was also the highest; thus, the BM treatment′s total net income decreased by 6.8% compared with the NM treatment. It is noteworthy that the grain yield and net income of the BM treatment were 0.6% and 14.0% lower than the PM treatment, respectively. Crop yields might be affected by the degradation materials that dominate the degradation behavior of biodegradable film. Li et al. [83] and Yin et al. [48] also demonstrated that biodegradable film with a faster or slower degradation rate seemed to reduce crop yields compared with those with a moderate degradation rate.

Importantly, from the environmentally friendly perspective, the substitution of polyethylene plastic film with biodegradable film to guarantee maize production and food security displayed great potential [84,85]. The study by Liu et al. [54] elaborated that the high price of biodegradable film is one of the factors limiting its large-scale promotion in China and emphasized the need to improve the production process of biodegradable film and reduce production costs on the one hand and to evaluate the comprehensive benefits of biodegradable film on the other. For this reason, we conducted a comprehensive benefits evaluation system of different film mulching patterns based on the AHP-GRA methods (Figure 2). It was found that the comprehensive benefits performance of BM treatment was better than the PM treatment (Figure 12), which is consistent with the results of numerous studies [86,87]. The economic benefits performance of the BM treatment was inferior to the PM and NM treatments, presenting a key obstacle to its large-scale promotion in China. Furthermore, the effect of the material cost of biodegradable film on the economic benefits was further investigated, as shown in Figure 14, which demonstrated that in this experiment, when the ratio of the BM and PM material cost was 1~1.37, the economic benefits of the BM treatment were higher than the NM treatment. However, the economic benefits of the BM treatment were higher than the PM treatment only when the ratio of the BM and PM material cost was 0.18. Therefore, reasonable control of material cost and improvement in the regional suitability of biodegradable film are essential for large-scale promotion.

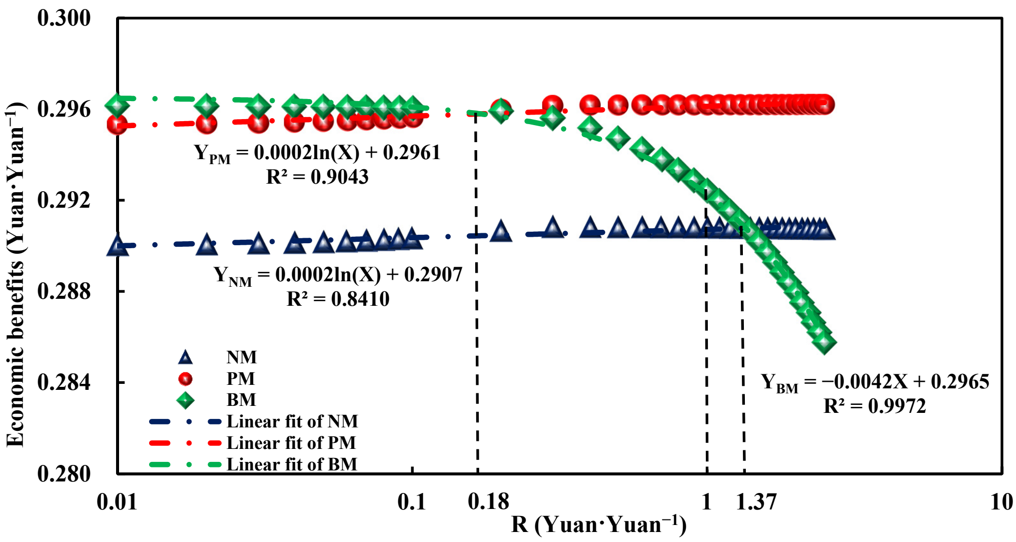

Figure 14. Evolution of economic benefits of NM, PM and BM treatments with the unit price ratio of BM to PM. R represents the ratio of material cost of BM to PM.

5. Conclusions

This study conducted a two-year experiment in a maize field in an arid region of northwest China to explore the coupling effects of different film mulching patterns and irrigation strategies in the agroecosystem. Furthermore, based on the economic, technical and ecological benefits, the comprehensive benefits under different film mulching patterns were evaluated by the AHP-GRA methods. The main conclusions were as follows:

(1) The FI treatment could accelerate the degradation of biodegradable film, which caused a significant increase in weight loss rate (6.1%) compared with the LI treatment.

(2) The difference in the accumulation of T_{s_PM}–T_{s_NM} and T_{s_BM}–T_{s_NM} was significant during the initial stage (0 to 30 DAS) and non-significant during the middle and late stages. The SEAT under the BM treatment was 150.3 °C (8.5%) higher than the NM treatment and 72.8 °C (4.1%) lower than the PM treatment.

(3) Film mulching could mitigate the negative impact of water deficit on crop yield, with the yield in BM and PM being enhanced by 11.6% and 18.6% compared with those in NM under the LI condition.

(4) Although PM showed the highest economic benefits, it had the lowest comprehensive benefits, followed by BM and NM. Only when the cost of BM material dropped to less than 1.37 times the cost of PM did the economic benefit of BM outcompete NM and result in a more acceptable and promising farming solution to boost environmental sustainability.

Author Contributions: Conceptualization, L.B. and X.M.; methodology, L.B.; formal analysis, L.B.; investigation, L.B. and Y.W.; writing—original draft preparation, L.B.; writing—review and editing, X.M.; supervision, X.M.; All authors have read and agreed to the published version of the manuscript.

Funding: This research was funded by the National Key Research and Development Program (No. 2021YFD1900801) and the National Natural Science Foundation of China (51790535, 51861125103).

Conflicts of Interest: The authors declare no conflict of interest.

References

1. Wang, J.Y.; Mo, F.; Nguluu, S.N.; Zhou, H.; Ren, H.X.; Zhang, J.; Li, F.M. Exploring micro-field water-harvesting farming system in dryland wheat (*Triticum aestivum* L.): An innovative management for semiarid Kenya. *Field Crop. Res.* **2016**, *196*, 207–218. [CrossRef]
2. Liao, Y.; Cao, H.X.; Xue, W.K.; Liu, X. Effects of the combination of mulching and deficit irrigation on the soil water and heat, growth and productivity of apples. *Agric. Water Manag.* **2021**, *243*, 106482. [CrossRef]
3. Bhardwaj, R.L. Effect of mulching on crop production under rainfed condition—A review. *Agric. Rev.* **2013**, *34*, 188–197. [CrossRef]
4. Zhao, Y.; Mao, X.M.; Shukla, M.K.; Tian, F.; Hou, M.J.; Zhang, T.; Li, S.E. How does film mulching modify available energy, evapotranspiration, and crop coefficient during the seed-maize growing season in northwest China? *Agric. Water Manag.* **2021**, *245*, 106666. [CrossRef]
5. Lin, W.; Liu, W.Z.; Zhou, S.S.; Liu, C.F. Influence of plastic film mulch on maize water use efficiency in the Loess Plateau of China. *Agric. Water Manag.* **2019**, *224*, 105710. [CrossRef]
6. Sun, D.B.; Li, H.G.; Wang, E.L.; He, W.Q.; Hao, W.P.; Yan, C.R.; Zhang, F.S. An overview of the use of plastic-film mulching in China to increase crop yield and water-use efficiency. *Natl. Sci. Rev.* **2020**, *7*, 1523–1526. [CrossRef] [PubMed]
7. National Bureau of Statistics of China. *China Agricultural Statistical Year Book*; China Statistics Press: Beijing, China, 2019.
8. Kasirajan, S.; Ngouajio, M. Polyethylene and biodegradable mulches for agricultural applications: A review. *Agron. Sustain. Dev.* **2012**, *32*, 501–529. [CrossRef]
9. Yang, N.; Sun, Z.X.; Feng, L.S.; Zheng, M.Z.; Chi, D.C.; Meng, W.Z.; Li, K.Y. Plastic film mulching for water-efficient agricultural applications and degradable films materials development research. *Mater. Manuf. Process.* **2014**, *30*, 143–154. [CrossRef]
10. Yan, C.R. Plastic-film mulch in Chinese agriculture: Importance and problems. *World Agric.* **2014**, *4*, 32–36.
11. Sintim, H.Y.; Flury, M. Is biodegradable plastic mulch the solution to agriculture's plastic problem? *Environ. Sci. Technol.* **2017**, *51*, 1068–1069. [CrossRef]
12. Yan, C.R.; Liu, E.K.; Shu, F.; Liu, Q.; Liu, S.; He, W.Q. Review of agricultural plastic mulching and its residual pollution and prevention measures in China. *J. Agric. Res. Environ.* **2014**, *31*, 95–102.
13. Jayasekara, R.; Harding, I.; Bowater, I.; Lonergan, G. Biodegradability of a selected range of polymers and polymer blends and standard methods for assessment of biodegradation. *J. Polym. Environ.* **2005**, *13*, 231–251. [CrossRef]
14. Kolybaba, M.; Tabil, L.G.; Panigrahi, S.; Crerar, W.J.; Powell, T.; Wang, B. Biodegradable polymers: Past, present, and future. In Proceedings of the ASABE/CSBE North Central Intersectional Meeting, Fargo, ND, USA, 3–4 October 2003.
15. Greer, L.; Dole, J.M. Aluminum foil, aluminium-painted, plastic, and degradable mulches increase yields and decrease insectvectored viral diseases of vegetables. *HortTechnology* **2003**, *13*, 276–284. [CrossRef]
16. Mooney, B.P. The second green revolution? Production of plant-based biodegradable plastics. *Biochem. J.* **2009**, *418*, 219–232. [CrossRef]

17. Ran, X.H.; Deng, P.Y.; Gang, Z.Y.; Dong, L.S. Characterization of full-biodegradable starch-PVA-polyester Film. *Chem. Res. Chin. Univ.* **2003**, *19*, 249–252.
18. Witt, U.; Einig, T.; Yamamoto, M.; Kleeberg, I.; Deckwer, W.D.; Muller, R.J. Biodegradation of aliphatic-aromatic copolyesters: Evaluation of the final biodegradability and ecotoxicological impact of degradation intermediates. *Chemosphere* **2001**, *44*, 289–299. [CrossRef]
19. Deng, L.; Yu, Y.; Zhang, H.Y.; Wang, Q.; Yu, R.D. The effects of biodegradable mulch film on the growth, yield, and water use efficiency of cotton and maize in an arid region. *Sustainability* **2019**, *11*, 7039. [CrossRef]
20. Yin, M.H.; Li, Y.N.; Li, H.; Xu, Y.B.; Zhang, T.L.; Gu, X.B. Effects of mulching patterns on farmland soil environment and winter wheat growth. *Trans. CSAM* **2016**, *47*, 127–135.
21. Wang, Z.H.; Wu, Q.; Fan, B.H.; Zheng, X.R.; Zhang, J.Z.; Li, W.H.; Guo, L. Effects of mulching biodegradable films under drip irrigation on soil hydrothermal conditions and cotton (*gossypium hirsutum* L.) yield. *Agric. Water Manag.* **2019**, *213*, 477–485. [CrossRef]
22. Zong, R.; Wang, Z.; Zhang, J.; Li, W. The response of photosynthetic capacity and yield of cotton to various mulching practices under drip irrigation in Northwest China. *Agric. Water Manag.* **2021**, *249*, 106814. [CrossRef]
23. Zhong, Y.; Fei, L.J.; Li, Y.B.; Zeng, J.; Dai, Z.G. Response of fruit yield, fruit quality, and water use efficiency to water deficits for apple trees under surge-root irrigation in the Loess Plateau of China. *Agric. Water Manag.* **2019**, *222*, 221–230. [CrossRef]
24. García, T.I.; Romero, V.R.; Jiménez, B.J.A.; Martínez, G.G.; Durán, Z.V.H.; Muriel, F.J.L. Response of citrus trees to deficit irrigation during different phenological periods in relation to yield, fruit quality, and water productivity. *Agric. Water Manag.* **2010**, *97*, 689–699. [CrossRef]
25. Chai, Q.; Gan, Y.; Zhao, C.; Xu, H.; Waskom, R.M.; Niu, Y.; Siddique, K.H.M. Regulated deficit irrigation for crop production under drought stress. A review. *Agron. Sustain. Dev.* **2015**, *36*, 3. [CrossRef]
26. Li, R.; Hou, X.Q.; Jia, Z.K.; Han, Q.F.; Ren, X.L.; Yang, B.P. Effects on soil temperature, moisture, and maize yield of cultivation with ridge and furrow mulching in the rainfed area of the Loess Plateau, China. *Agric. Water Manag.* **2013**, *116*, 101–109. [CrossRef]
27. Sun, T.; Li, G.; Ning, T.Y.; Zhang, Z.M.; Mi, Q.H.; Lal, R. Suitability of mulching with biodegradable film to moderate soil temperature and moisture and to increase photosynthesis and yield in peanut. *Agric. Water Manag.* **2018**, *208*, 214–223. [CrossRef]
28. Zhang, X.F.; Luo, C.L.; Ren, H.X.; Dai, R.Z.; Mburu, D.; Kavagi, L.; Xiong, Y.C. Fully biodegradable film to boost rainfed maize (*Zea mays* L.) production in semiarid Kenya: An environmentally friendly perspective. *Eur. J. Agron.* **2020**, *119*, 126124. [CrossRef]
29. Menossi, M.; Cisneros, M.; Alvarez, V.A.; Casalongué, C. Current and emerging biodegradable mulch films based on polysaccharide bio-composites. A review. *Agron. Sustain. Dev.* **2021**, *41*, 41–53. [CrossRef]
30. Cui, L.Y.; Zhang, Y.S.; Jin, H.; Ma, X. Safety evaluation of chemical production based on AHP-fuzzy comprehensive evaluation method. In Proceedings of the IOP Conference Series: Earth and Environmental Science, Arpad Horvath, University of California, Berkeley, CA, USA, 12 December 2021.
31. Si, T.; Wang, C.B.; Liu, R.; Guo, Y.S.; Yue, S.; Ren, Y.J. Multi-criteria comprehensive energy efficiency assessment based on fuzzy-AHP method: A case study of post-treatment technologies for coal-fired units. *Energy* **2020**, *200*, 117533. [CrossRef]
32. Hu, J.; Chen, J.; Chen, Z.; Cao, J.X.; Wang, Q.F.; Zhao, L.B.; Chen, G.D. Risk assessment of seismic hazards in hydraulic fracturing areas based on fuzzy comprehensive evaluation and AHP method (FAHP): A case analysis of Shangluo area in Yibin City, Sichuan Province, China. *J. Pet. Sci. Eng.* **2018**, *170*, 797–812. [CrossRef]
33. Saaty, T.L. A scaling method for priorities in hierarchical structures. *J. Math. Psychol.* **1977**, *15*, 234–281. [CrossRef]
34. Han, Y.M.; Zhou, R.D.; Geng, Z.Q.; Bai, J.; Ma, B.; Fan, J.Z. A novel data envelopment analysis cross-model integrating interpretative structural model and analytic hierarchy process for energy efficiency evaluation and optimization modeling: Application to ethylene industries. *J. Clean. Prod.* **2020**, *246*, 118965. [CrossRef]
35. Heindl, A.-B.; Liefner, I. The Analytic Hierarchy Process as a methodological contribution to improve regional innovation system research: Explored through comparative research in China. *Technol. Soc.* **2019**, *59*, 101197. [CrossRef]
36. Li, B.; Chen, Y.L. Risk assessment of coal floor water inrush from underlying aquifers based on GRA-AHP and its application. *J. Geotech. Geoenviron. Eng.* **2016**, *34*, 143–154. [CrossRef]
37. Zhang, J.; Yang, T. Study of a roof water inrush prediction model in shallow seam mining based on an analytic hierarchy process using a grey relational analysis method. *Arab. J. Geosci.* **2018**, *11*, 153. [CrossRef]
38. Jiang, H.P.; Huang, D.L. Econometrics evalution of China agricultural modernization. *Res. Agric. Moderni.* **2006**, *27*, 87–91.
39. Wang, H.; Cheng, M.; Zhang, S.; Fan, J.; Feng, H.; Zhang, F.; Xiang, Y. Optimization of irrigation amount and fertilization rate of drip-fertigated potato based on Analytic Hierarchy Process and Fuzzy Comprehensive Evaluation methods. *Agric. Water Manag.* **2021**, *256*, 107130. [CrossRef]
40. He, Q.S.; Li, S.E.; Kang, S.Z.; Yang, H.B.; Qin, S.J. Simulation of water balance in a maize field under film-mulching drip irrigation. *Agric. Water Manag.* **2018**, *210*, 252–260. [CrossRef]
41. Moreno, M.M.; Moreno, A. Effect of different biodegradable and polyethylene mulches on soil properties and production in a tomato crop. *Sci. Hortic.* **2008**, *116*, 256–263. [CrossRef]
42. Ran, H.; Kang, S.Z.; Hu, X.T.; Li, S.E.; Wang, W.; Liu, F.L. Capability of a solar energy-driven crop model for simulating water consumption and yield of maize and its comparison with a water-driven crop model. *Agric. For. Meteorol.* **2020**, *287*, 107955. [CrossRef]

43. Allen, R.G.; Pereira, L.S.; Raes, D.; Smith, M. Crop evapotranspiration-guidelines for computing crop water requirements. In *FAO Irrigation and Drainage Paper 56*; Food and Agriculture Organization of United Nations: Rome, Italy, 1998.
44. Zhang, S.; Gao, P.; Tong, Y.; Norse, D.; Lu, Y.; Powlson, D. Overcoming nitrogen fertilizer over-use through technical and advisory approaches: A case study from Shaanxi Province, northwest China. *Agric. Ecosyst. Environ.* **2015**, *209*, 89–99. [CrossRef]
45. Wang, S.; Luo, S.; Yue, S.; Shen, Y.; Li, S. Fate of 15N fertilizer under different nitrogen split applications to plastic mulched maize in semiarid farmland. *Nutr. Cycl. Agroecosystems* **2016**, *105*, 129–140. [CrossRef]
46. Yin, G.; Gu, J.; Zhang, F.; Hao, L.; Cong, P.; Liu, Z. Maize yield response to water supply and fertilizer input in a semi-arid environment of Northeast China. *PLoS ONE* **2014**, *9*, e86099. [CrossRef] [PubMed]
47. Faloye, O.T.; Alatise, M.O.; Ajayi, A.E.; Ewulo, B.S. Synergistic effects of biochar and inorganic fertiliser on maize (*zea mays*) yield in an alfisol under drip irrigation. *Soil Tillage Res.* **2017**, *174*, 214–220. [CrossRef]
48. Yin, M.H.; Li, Y.N.; Fang, H.; Chen, P.P. Biodegradable mulching film with an optimum degradation rate improves soil environment and enhances maize growth. *Agric. Water Manag.* **2019**, *216*, 127–137. [CrossRef]
49. Wang, Z.H.; Wu, Q.; Fan, B.H.; Zhang, J.; Li, W.H.; Zheng, X.R.; Guo, L. Testing biodegradable films as alternatives to plastic films in enhancing cotton (*Gossypium hirsutum* L.) yield under mulched drip irrigation. *Soil Tillage Res.* **2019**, *192*, 196–205. [CrossRef]
50. Yang, H.D.; Tang, S.Z. Evaluating method for testing of degradable plastics. *Plastics* **1996**, *25*, 16–21.
51. Ren, X.L.; Chen, X.L.; Cai, T.; Wei, T.; Wu, Y.; Ali, S.; Jia, Z.K. Effects of ridge-furrow system combined with different degradable mulching materials on soil water conservation and crop production in semi-humid areas of China. *Front. Plant. Sci.* **2017**, *8*, 1877. [CrossRef]
52. Fernández, J.E.; Alcon, F.; Diaz-Espejo, A.; Hernandez-Santana, V.; Cuevas, M.V. Water use indicators and economic analysis for on-farm irrigation decision: A case study of a super high density olive tree orchard. *Agric. Water Manag.* **2020**, *237*, 106074. [CrossRef]
53. Wang, Y.Z.; Yang, K.K.; Wang, X.L.; Zhou, Q.; Zheng, C.Y.; Chen, Z.F. Agricultural application and environmental degradation of photo-biodegradable polyethylene mulching films. *J. Polym. Environ.* **2004**, *12*, 7–10. [CrossRef]
54. Liu, E.K.; Zhang, L.W.; Dong, W.Y.; Yan, C.R. Biodegradable plastic mulch films in agriculture: Feasibility and challenges. *Environ. Res. Lett.* **2021**, *16*, 011004. [CrossRef]
55. Sintim, H.Y.; Bary, A.I.; Hayes, D.G.; Wadsworth, L.C.; Anunciado, M.B.; English, M.E.; Flury, M. In situ degradation of biodegradable plastic mulch films in compost and agricultural soils. *Sci. Total Environ.* **2020**, *727*, 138668. [CrossRef]
56. Gu, X.B.; Cai, H.J.; Fang, H.; Chen, P.P.; Li, Y.P.; Li, Y.N. Soil hydro-thermal characteristics, maize yield and water use efficiency as affected by different biodegradable film mulching patterns in a rain-fed semi-arid area of China. *Agric. Water Manag.* **2021**, *245*, 106560. [CrossRef]
57. Kapanen, A.; Schettini, E.; Vox, G.; Itävaara, M. Performance and environmental impact of biodegradable films in agriculture: A field study on protected cultivation. *J. Polym. Environ.* **2008**, *16*, 109–122. [CrossRef]
58. Kitamoto, H.; Yoshida, S.; Koitabashi, M.; Yamamoto-Tamura, K.; Ueda, H.; Yarimizu, T.; Sameshima-Yamashita, Y. Enzymatic degradation of poly-butylene succinate-co-adipate film in rice husks by yeast Pseudozyma antarctica in indoor conditions. *J. Biosci. Bioeng.* **2018**, *125*, 199–204. [CrossRef]
59. Rafael, A.; Bruce, H.; Susan, S. An overview of polylactides as packaging materials. *Macromol. Biosci.* **2004**, *4*, 835–864.
60. Shen, L.X.; Wang, P.; Zhang, L.L. Effects of degradable film on soil temperature, moisture and growth of maize. *Trans. CSAE* **2012**, *24*, 111–116.
61. Chen, N.; Li, X.Y.; Shi, H.B.; Hu, Q.; Zhang, Y.H.; Sun, Y.N.; Song, F.F. Simulation of maize crop growth using an improved crop model considering the disintegrated area of biodegradable film. *Field Crop. Res.* **2021**, *272*, 108270. [CrossRef]
62. Pramanik, P.; Bandyopadhyay, K.K.; Bhaduri, D.; Bhattacharyya, R.; Aggarwal, P. Effect of mulch on soil thermal regimes—A review. *Int. J. Agric. Biotechnol. Food Sci.* **2015**, *8*, 667–681. [CrossRef]
63. Zhou, L.M.; Jin, S.L.; Liu, C.A.; Xiong, Y.C.; Si, J.T.; Li, X.G.; Li, F.M. Ridge-furrow and plastic-mulching tillage enhances maize–soil interactions, Opportunities and challenges in a semiarid agroecosystem. *Field Crop. Res.* **2012**, *126*, 181–188. [CrossRef]
64. Li, X.Y.; Peng, Z.Y.; Shi, H.B.; Yan, J.W.; Wang, Z.C. Effects of different degradable films mulching on soil water potential, temperature and sunflower growth. *Trans. CSAM* **2015**, *46*, 97–103.
65. Gu, X.B.; Li, Y.N.; Du, Y.D. Biodegradable film mulching improves soil temperature, moisture and seed yield of winter oilseed rape (*Brassica napus* L.). *Soil Tillage Res.* **2017**, *171*, 42–50. [CrossRef]
66. Gan, Y.T.; Siddique, K.H.M.; Turner, N.C.; Li, X.G.; Niu, J.Y.; Yang, C.; Chai, Q. Ridge-furrow mulching systems—An Innovative technique for boosting crop productivity in semiarid rain-fed environments. *Adv. Agron.* **2013**, *118*, 429–476. [CrossRef]
67. Sarkar, S.; Paramanick, M.; Goswami, S.B. Soil temperature, water use and yield of yellow sarson (*Brassica napus* L. var. *glauca*) in relation to tillage intensity and mulch management under rainfed lowland ecosystem in eastern India. *Soil Tillage Res.* **2007**, *93*, 94–101. [CrossRef]
68. Wu, Y.; Huang, F.Y.; Jia, Z.K.; Ren, X.L.; Cai, T. Response of soil water, temperature, and maize (*Zea may* L.) production to different plastic film mulching patterns in semi-arid areas of northwest China. *Soil Tillage Res.* **2017**, *166*, 113–121. [CrossRef]
69. Zhao, Y.; Mao, X.M.; Shukla, M.K. A modified SWAP model for soil water and heat dynamics and seed-maize growth under film mulching. *Agric. For. Meteorol.* **2020**, *292–293*, 108127. [CrossRef]
70. Gong, D.Z.; Mei, X.R.; Hao, W.P.; Wang, H.B.; Caylor, K.K. Comparison of ET partitioning and crop coefficients between partial plastic mulched and non-mulched maize fields. *Agric. Water Manag.* **2017**, *181*, 23–34. [CrossRef]

71. Ding, R.S.; Kang, S.Z.; Li, F.S.; Zhang, Y.Q.; Tong, L. Evapotranspiration measurement and estimation using modified Priestley–Taylor model in an irrigated maize field with mulching. *Agric. For. Meteorol.* **2013**, *168*, 140–148. [CrossRef]
72. Kang, S.Z.; Gu, B.J.; Du, T.S.; Zhang, J.H. Crop coefficient and ratio of transpiration to evapotranspiration of winter wheat and maize in a semi-humid region. *Agric. Water Manag.* **2003**, *59*, 239–254. [CrossRef]
73. Shen, Q.X.; Ding, R.S.; Du, T.S.; Tong, L.; Li, S.E. Water use effectiveness is enhanced using film mulch through increasing transpiration and decreasing evapotranspiration. *Water* **2019**, *11*, 1153. [CrossRef]
74. Zhang, Y.Q.; Wang, J.D.; Gong, S.H.; Xu, D.; Sui, J.; Wu, Z.D.; Mo, Y. Effects of film mulching on evapotranspiration, yield and water use efficiency of a maize field with drip irrigation in Northeastern China. *Agric. Water Manag.* **2018**, *205*, 90–99. [CrossRef]
75. Chen, Y.L.; Liu, T.; Tian, X.H.; Wang, X.F.; Li, M.; Wang, S.X.; Wang, Z.H. Effects of plastic film combined with straw mulch on grain yield and water use efficiency of winter wheat in Loess Plateau. *Field Crop. Res.* **2015**, *172*, 53–58. [CrossRef]
76. Mo, F.; Wang, J.Y.; Zhou, H.; Luo, C.L.; Zhang, X.F.; Li, X.Y.; Xiong, Y.C. Ridge-furrow plastic-mulching with balanced fertilization in rainfed maize (*Zea mays* L.): An adaptive management in east African Plateau. *Agric. For. Meteorol.* **2017**, *236*, 100–112. [CrossRef]
77. Abduwaiti, A.; Liu, X.W.; Yan, C.R.; Xue, Y.H.; Jin, T.; Wu, H.Q.; Liu, Q. Testing biodegradable films as alternatives to plastic-film mulching for enhancing the yield and economic benefits of processed tomato in Xinjiang region. *Sustainability* **2021**, *13*, 3093. [CrossRef]
78. Ida, D.M.; Eugenio, C.; Lucia, O.; Giuseppe, D.L.; Riccardo, R.; Patrizia, S.; Mauro, M. The effect of novel biodegradable films on agronomic performance of zucchini squash grown under open-field and greenhouse conditions. *Aust. J. Crop. Sci.* **2019**, *13*, 1810–1818. [CrossRef]
79. Maria, G.; Amoroso, C.; Christophe, E.-N.; Rouphael, Y.; Stefania, D.P.; Cirillo, C. An appraisal of biodegradable mulch films with respect to strawberry crop performance and fruit quality. *Horticulturae* **2020**, *6*, 48.
80. Braunack, M.V.; Adhikari, R.; Freischmidt, G.; Johnston, P.; Casey, P.S.; Wang, Y.; Filipović, V. Initial experimental experience with a sprayable biodegradable polymer membrane (SBPM) technology in cotton. *Agron. J.* **2020**, *10*, 584. [CrossRef]
81. Alam, M.A.; Seetharam, K.; Zaidi, P.H.; Dinesh, A.; Vinayan, M.T.; Nath, U.K. Dissecting heat stress tolerance in tropical maize (*Zea mays* L.). *Field Crop. Res.* **2017**, *204*, 110–119. [CrossRef]
82. Oury, V.; Tardieu, F.; Turc, O. Ovary apical abortion under water deficit Is caused by changes in sequential development of ovaries and in silk growth rate in maize. *Plant. Physiol.* **2016**, *171*, 986–996.
83. Li, C.; Moore-Kucera, J.; Lee, J.; Corbin, A.; Brodhagen, M.; Miles, C.; Inglis, D. Effects of biodegradable mulch on soil quality. *Appl. Soil Ecol.* **2014**, *79*, 59–69. [CrossRef]
84. Costa, R.; Saraiva, A.; Carvalho, L.; Duarte, E. The use of biodegradable mulch films on strawberry crop in Portugal. *Sci. Hortic.* **2014**, *173*, 65–70. [CrossRef]
85. Gordon, C.; Gary, T. Science for African Food Security. *Science* **2003**, *299*, 1187–1188.
86. Wortman, S.E.; Kadoma, I.; Crandall, M.D. Assessing the potential for spunbond, nonwoven biodegradable fabric as mulches for tomato and bell pepper crops. *Sci. Hortic.* **2015**, *193*, 209–217. [CrossRef]
87. Zhang, X.Y.; You, S.Y.; Tian, Y.Q.; Li, J.S. Comparison of plastic film, biodegradable paper and bio-based film mulching for summer tomato production: Soil properties, plant growth, fruit yield and fruit quality. *Sci. Hortic.* **2019**, *249*, 38–48. [CrossRef]